

APPLICATION OF HOLOGRAPHIC INTERFEROMETRY TO
SUPERSONIC FLOW VISUALIZATION OF A REAR-FACING
STEP AND APPLICATION OF FAST FOURIER TRANSFORM
METHODS TO CURRENT DATA REDUCTION TECHNIQUES

Harland Wilber Jones

DUDLEY KNOX LIBRARY
NAVAL POSTGRADUATE SCHOOL
MONTEREY, CALIFORNIA 93940

NAVAL POSTGRADUATE SCHOOL

Monterey, California



THESIS

APPLICATION OF HOLOGRAPHIC INTERFEROMETRY TO
SUPERSONIC FLOW VISUALIZATION OF A REAR-FACING
STEP AND APPLICATION OF FAST FOURIER TRANSFORM
METHODS TO CURRENT DATA REDUCTION TECHNIQUES

by

Harland Wilber Jones, Jr.

Thesis Advisor:

D. J. Collins

March 1974

T160136

Approved for public release; distribution unlimited.

Application of Holographic Interferometry to
Supersonic Flow Visualization of a Rear-Facing
Step and Application of Fast Fourier Transform
Methods to Current Data Reduction Techniques

by

Harland Wilber Jones, Jr.
Lieutenant, United States Navy
B.S., United States Naval Academy, 1968

Submitted in partial fulfillment of the
requirements for the degree of

MASTER OF SCIENCE IN AERONAUTICAL ENGINEERING

from the

NAVAL POSTGRADUATE SCHOOL
March 1974

ABSTRACT

The successful application of holographic interferometry to the study of three-dimensional density fields around bodies in wind tunnel experiments has been reported in the literature along with the associated mathematical reduction processes for the basic interferometric equation.

The present report has extended the application of holography as a flow visualization technique by investigating Mach 2.8 flow over a rear-facing $1/8$ in. step. Two single-exposed holograms of the model and two double-exposed frozen fringe holographic interferograms of the flow were created.

Fast Fourier Transform (FFT) methods have been reported as significantly reducing computational time to obtain discrete and inverse discrete Fourier transforms. Two computer programs were designed to apply FFT methods to the Fourier transform approach to the basic interferometric equation. These programs were used to investigate an alternate way to calculate the value of the inside integral. Total agreement was not found, and further analysis as to the accuracy of each method is needed.

TABLE OF CONTENTS

I.	INTRODUCTION.....	9
II.	INTRODUCTION TO HOLOGRAPHY.....	10
III.	INVESTIGATION OF A REAR-FACING STEP.....	12
IV.	EXPERIMENTAL MODEL.....	13
V.	DESCRIPTION OF APPARATUS.....	14
VI.	EXPERIMENTAL PROCEDURE.....	15
VII.	FILM AND DEVELOPMENT PROCEDURE.....	16
VIII.	RECONSTRUCTION TECHNIQUE, EQUIPMENT, AND RESULTS.....	17
IX.	CURRENT DATA REDUCTION TECHNIQUES.....	19
X.	APPLICATION OF THE FAST FOURIER TRANSFORM.....	24
XI.	RESULTS AND RECOMMENDATIONS FOR FFT APPLICATION.....	28
XII.	SUMMARY OF RESULTS.....	30
	FIGURES.....	31
	APPENDIX A: Detailed Experimental Procedures.....	43
	APPENDIX B: The Inside Integral Subsection Of Van Houten's Computer Program.....	45
	APPENDIX C: FFT Convolution Procedures:	
	1. Computation Procedure For FFT Convolution Of Finite-Length Functions.....	46
	2. Computation Procedure For FFT Convolution: Select-Savings Method.....	47
	3. Computation Procedure For FFT Convolution: Overlap-Add Method.....	48
	APPENDIX D: SUBROUTINE CFFT2.....	49
	APPENDIX E: MODE1--Mode One Operation Of Van Houten's Computer Program With Some Modifications.....	67

APPENDIX F: Alternate Programs Designed To Calculate The Value Of The Inside Integral:	
1. JONES1--Using Convolution Values Obtained Numerically.....	78
2. JONES2--Using Convolution Values Obtained With FFT Methods.....	80
3. Listing Of The Expanded Fringe Shift Information Values Supplied To Both JONES1 And JONES2.....	83
APPENDIX G: Comparison Of JONES1 And JONES2 Values Of The Inside Integral With Van Houten's Values Of The Inside Integral.....	85
REFERENCES.....	86
INITIAL DISTRIBUTION LIST.....	88
FORM DD 1473.....	89

LIST OF FIGURES

1. Chapman-Korst Flow Model for Supersonic Base Flow.....	31
2. Lip Shock.....	32
3. The Experimental Model of a Rear-Facing Step.....	33
4. Experimental Model.....	34
5. Experimental Setup.....	35
6. A View of the Left Side of the Experimental Setup Showing the Laser and the Optics System up to the Beam Splitter.....	36
7. View of the Left Side of the Test Section, also Showing the Q-Switched Laser, the Beam Splitter, and Mirrors which Direct the Reference Beam over the Test Section.....	36
8. A View of the Right Side of the Test Section.....	37
9. A View of the Right Side of the Experimental Setup Showing the Holographic Plane and the Final Mirrors for the Reference and the Scene Beams.....	37
10. Reconstruction Setup.....	38
11. Photograph of the Projected Real Image of a Single-Exposed Hologram.....	39
12. Photograph of the Projected Real Image of a Single-Exposed Hologram.....	39
13. Photograph of the Projected Real Image of a Double-Exposed Hologram of a Rear-Facing 1/8 in. Step in Mach 2.8 Flow.....	40
14. Photograph of the Projected Real Image of a Double-Exposed Hologram of a Rear-Facing 1/8 in. Step in Mach 2.8 Flow.....	40
15. The Number of Operations Required to Compute the Discrete Fourier Transform by Direct Calculation Compared with Using the FFT Algorithm.....	41
16. Optimum Value of N for FFT Convolution.....	42

TABLE OF SYMBOLS

Symbol	Meaning
DFT	Discrete Fourier transform
DR	Interval between frequency plane values, used as a weighting function for determining the convolution
$F(A)$	Operator meaning "to take the discrete Fourier transform of 'A'"
$F^{-1}(A)$	Operator meaning "to take the inverse discrete Fourier transform of 'A'"
FFT	Fast Fourier transform
IDFT	Inverse discrete Fourier transform
L	Length
M	Mach number
mW	Milliwatt
n, n_0	Index of refraction, reference index of refraction
NP	Number of points of frequency plane values
Q	Number of frequency plane values in the finite sample
r	Radius
R	Radius of convolution vector
RMAX	Maximum radius of original finite frequency plane values
S_i	The i^{th} region of integration
dS_i	Distance along the i^{th} ray traversing the test section
t	Step size of rear-facing step
U	Local velocity
\AA	Angstrom degree, equal to 10^{-8} cm.
γ	Power of 2, i.e. 2^γ
$(C1 * C2)$	"*" Operator meaning "C1 is convoluted with C2"

$\frac{\partial(a)}{\partial b}$	Operator meaning the "partial derivative of 'a' with respect to 'b'"
θ	Angular measurement in polar coordinates
ν	Coefficient of viscosity for fluid involved in the flow under consideration
φ	View angle
ρ_i	Known path length function; frequency plane values
ρ	Distance from origin in polar coordinates
ρ, ρ_0	Density, reference density

ACKNOWLEDGMENTS

The writer wishes to gratefully acknowledge Dr. D. J. Collins for his most valuable guidance and assistance throughout the course of this investigation; the technical staff of the Department of Aeronautics under R. Besel and T. Dunton, particularly N. Leckenby for his invaluable assistance in construction and operation of the experimental equipment and G. Middleton for his fabrication of the experimental model; Deborah Janov for her considerable effort in the final preparation and typing of this report; and my wife and family for their noble patience and encouragement.

I. INTRODUCTION

This thesis contains both an experimental section and a theoretical section. The experimental portion involved the construction of a modified Z-type Schlieren system to conduct holographic investigation of a rear-facing step in supersonic flow. The theoretical portion involved investigating current data reduction techniques for determining the three-dimensional distribution of a field by applying fast Fourier transform methods to solve the basic interferometric equation. Two original computer programs were devised in an attempt to reduce computer computational time required for interferometric data reduction.

II. INTRODUCTION TO HOLOGRAPHY

Holography is a three-dimensional photography-like process which involves the recording of both phase and amplitude information of light waves diffracted by an object illuminated with coherent light. Originally proposed by Gabor [1,2] in 1948, holography awaited the development of the laser around 1960 to become an explosive field of its own. The laser contributed a basically monochromatic, coherent light source. The property of coherence, or the capability of interference with itself, enables the recording of both phase and amplitude information.

Photography records the intensity of illumination, which is the time average of the square of the amplitude of the light field at any point. In holography, a coherent light beam is separated into a reference beam and an object (or scene) beam. The reference beam is directed to the holographic plane via an optics system while the object beam reaches the same point after being diffracted by a subject of interest. The emulsion on the holographic plate records the intensities of the illuminating beams and the interference between the two beams. The interference component contains the phase information which permits reconstruction of an image possessing full three-dimensionality and parallax properties. No attempt will be made to present the full mathematical and historical development of holography which is amply done in many excellent texts. [3]

Among its many engineering applications, holography is well suited for flow visualization. Recent successful applications of holography at the Naval Postgraduate School include the study of a free jet and the determination of the density field about a cone tilted in supersonic flow in a conventional wind tunnel. The use of double-pulsed holography is

especially helpful as a tool for measurement in high velocity flows near vibrating equipment such as free jets and blow-down wind tunnels. A Q-switch ruby laser is used as a high power energy source emitting a coherent light pulse on the order of several joules in an extremely small time span, on the order of twenty nanoseconds. Vibrations of the object or of the optical system components, which must remain stable within wave lengths of light during exposure of the hologram, are of negligible importance due to the very short duration of the exposure time.

A double-pulsed (or double-exposed) approach is advantageous in flow visualization. In the Mach-Zender interferometer, comparison of the reference and object beams are made at the same time. With holography it is possible to separate the simultaneous comparison in time. Two holograms, or exposures, are made on the same holographic plate without intermediate development. The first exposure is made with no flow and the second with flow. The individual holograms interfere with each other, creating an interferogram of the flow. Essentially, this interferogram contains only the differences in optical path lengths between the two exposures. Therefore, any imperfections in optical components, (which are identical for both exposures), are subtracted out, thereby eliminating the need for high quality optics [4].

Another method of taking finite fringe holograms is the double-exposure option of the dual hologram method, which involves using two holographic plates. One plate is used for each exposure. A dual hologram holder positions each plate in the same location for its exposure. The improvement comes from the versatility of almost an infinite set of reconstruction possibilities from one set of plates. A dual hologram holder has recently been constructed at the Naval Postgraduate School to demonstrate its application. This topic was the subject of AIAA Paper 73-210 [5].

III. INVESTIGATION OF A REAR-FACING STEP

Holographic investigation of a rear-facing step in supersonic flow was selected for two main reasons. First, extensive theoretical and experimental investigations of a rear-facing step in two-dimensional supersonic flow are available. This provides ample information for verifying results from this experiment. Secondly, previous experimental results do not completely agree with theoretical descriptions. A source of conflict is the lip shock's influence on the rest of the flow as it pertains to the reattachment point and to the tail shock. With this in mind, it was hoped to provide a hologram which could be used to accurately reproduce the flow field.

The classical flow model for supersonic base flow, (rear-facing step flow), was proposed by Chapman [6] in 1957 and independently by Korst [7] for turbulent flow, and is commonly known as the Chapman-Korst flow model. Refer to Figure 1 for a sketch of the Chapman-Korst flow model. Roache [8] presented a literature search and a review of discrepancies with this model in his doctoral thesis for the University of Michigan in 1968. The main, unresolved discrepancies in the Chapman-Korst flow model were: that the experimental pressure at recompression was not equal to the theoretical pressure of Region Four (see Fig. 1); and that the isentropic turn from Regions One to Two (see Fig. 1) and the constant pressure assumptions were invalidated by the presence of the lip shock (see Fig. 2) at higher Mach numbers. [9]

The opportunity to provide some accurate data on these unresolved areas of interest appeared to be a worthwhile application of holography.

IV. EXPERIMENTAL MODEL

The actual rear-facing step model used was limited in size, with the maximum step size being one-eighth inch. Due to the small step size, the boundary layer thickness (δ) was compared with the step size (t) to determine if distortions from the boundary layer would invalidate experimental results. From Schlichting [10], the applicable equations are: $\delta = 5 (\nu L / U)^{\frac{1}{2}}$ for laminar flow; and $\delta / L = .37 (U L / \nu)^{-1/5}$ for the boundary layer thickness at the trailing edge of a flat plate at zero incidence in parallel turbulent flow. The δ / t ratio results were .0538 for laminar flow and .218 for turbulent flow. It was felt that the actual flow situation was laminar and that this step size would still offer meaningful results.

A photograph of the model is included as Figure 3. Refer to Figure 4 for a sketch showing the dimensions of the model.

V. DESCRIPTION OF APPARATUS

Figure 5 shows a complete sketch of the experimental setup. A modified Z-type Schlieren system, it was constructed specifically for this thesis. A description of the integrated setup will be followed by listing of important supportive equipment.

A high energy pulse was discharged from a Q-switch ruby laser and passed through a diffusing lens to a collimating mirror in order to expand the light beam to sufficiently illuminate the test section. The collimated beam reflected off a flat mirror towards the test section. Just prior to the test section, the beam was divided by a beam splitter mounted on a tripod. The object (scene) beam transmitted through the beam splitter, through the test section, and reflected off another flat mirror towards a converging mirror. The object beam was then reflected towards the holographic plane which was positioned in the diverging part of the beam where the test object was in focus. The part of the collimated beam reflected by the beam splitter, the reference beam, reflected off three flat mirrors and also illuminated the holographic plane.

Other equipment included an air supply for the tunnel provided by an air compressor; a power supply and cooling system for the laser; a 15 mW continuous wave Helium-Neon laser used for alignment of the Q-switched ruby laser with the optics system; an autocollimator for internal alignment of the Q-switch laser; a movable platform for the laser so it can be elevated to the proper height for the optics system; a table for the hologram holder; and mountings and supports for all optic components. Figures 6-9 are pictures showing the experimental setup from four different views.

Safety equipment included eye protectors and sound attenuators.

VI. EXPERIMENTAL PROCEDURE

Appendix A contains a detailed description of the entire experimental procedure from alignment of system components to exposure of various types of holograms.

There are two holographic methods that can be applied to flow visualization in wind tunnels. The first method is commonly referred to as the real fringe method, and the second as the frozen fringe or double-exposed method.

Real fringe methods require exposure of the holographic plate with no flow in the wind tunnel and either development of the hologram in place or precise repositioning of the developed plate. As flow is increased in the wind tunnel, an evolution of real fringe patterns could be observed through the hologram. This method was not used in this experiment due to the unavailability of in-place developing equipment or a dual-hologram holder.

Double-exposed or frozen fringe methods require two exposures of the same holographic plate. The first exposure is taken with no flow in the wind tunnel, and the second with flow. The interference between the two exposures results in a double-pulsed (exposed) interferogram. In this experiment both exposures were made on the same plate with the second exposure occurring while Mach 2.8 flow existed in the test section.

VII. FILM AND DEVELOPMENT PROCEDURE

There are essentially two sources of holographic films: Eastman Kodak Company and Agfa-Gevaert. Agfa-Gevaert films were used exclusively in this experiment because their 75 series film is designed for maximum sensitivity around the emission spectrum of ruby lasers (6943 Å). Due to the short duration of the exposure time of the Q-switch ruby laser, about 10-20 nanoseconds, 10E75 film was used because 8E75 film turned out to be too slow in recording information.

Development of holograms can include various features such as bleaching, prehardening, or varying development time. The various alternatives are examined in Ref. 11. For this experiment the following development procedure was used:

1. Five minutes in Kodak D-19 Developer
2. Thirty seconds in an acetic acid stop bath of standard dilution.
3. Five minutes in a standard fixer.
4. Five minutes of washing followed by immersion in a wetting agent (Kodak Photoflo) prior to drying.

VIII. RECONSTRUCTION TECHNIQUE, EQUIPMENT, AND RESULTS

A 15 mW continuous wave Helium-Neon laser, previously used for alignment, was the coherent light source used for reconstruction. A collimating lens was attached to this laser in order to expand the reconstruction beam to approximately two inches. Other reconstruction equipment included a hologram holder, type 52P Polaroid film, a graphic view camera, a tripod, and a black drape.

The two-inch diameter collimated beam incident to the hologram created two images. Whether projected images are real or virtual is discussed in Chapter 3 of Ref. 3 for the various combinations of converging, diverging, and collimated reference and scene beams. In this experiment, approximate symmetry about the vertical axis of the holographic plate was attempted. This resulted in the real image being projected as a converging wave front and in the virtual image being projected as a diverging wave front.

In order to focus the real image, the lens was removed from a camera and the image was projected on the ground glass backing of the camera. Pictures of these projections were taken at exposure times which varied with the intensity of the real image beam. Normal exposure times were approximately one second.

Figure 10 is a sketch of the reconstruction setup and Figures 11-14 are examples of photographs of the projections of the real image of holograms taken with this experimental setup.

Figures 13 and 14 represent the final experimental attempts to create a frozen fringe hologram of sufficient quality to warrant data reduction. The edges of the experimental model show that both holograms are slightly out of focus. These holograms were, however, sufficient to demonstrate

the applicability of holography to flow visualization of a rear-facing step in supersonic flow. Additionally, the shadowgraph resulting on the developed plate showed the basic features of the Chapman-Korst flow model. Sufficient information was not obtained to analyze any of previously mentioned discrepancies of that model.

The remaining effort of this thesis focused on the possibilities of improving current data reduction methods.

IX. CURRENT DATA REDUCTION TECHNIQUES

There are currently several approaches for reducing an asymmetric density field. One method involves a series expansion of a complete set of orthogonal polynomials which are invariant to a rotation of coordinates [12]. Matulka, [13] used this method and created a computer program which took approximately two hours of computer time to reduce the data for the asymmetric case.

A second approach uses Fourier transform techniques suggested by Rowley [14] and further developed by Junginger and van Haeringen [15]. This approach is thoroughly discussed by Sweeney [16] in his doctoral thesis for the University of Michigan in 1972.

Closely following Sweeney's development and nomenclature, the fundamental integral equation to be solved in three-dimensional interferometry is

$$\int_{S_i} f(x,y,z) dS_i = \phi_i \quad (9-1)$$

where $f(x,y,z)=n(x,y,z)-n_0$; $f(x,y,z)$ is the refractive index relative to a known value n_0 , S_i is the distance along the i^{th} ray traversing the test section, ϕ_i is the known path length function, and the integral is evaluated between boundaries imposed by experimental configuration or by prior knowledge regarding $f(x,y,z)$. The objective is to reconstruct a real scalar function, the relative refractive index field, from the scalar values of line integrals through the field. When the gradient of the refractive index variation is small enough to produce negligible ray curvature, eqn. (9-1) alone is the basic interferometric equation to be solved. The line integrals are then evaluated along straight, not curved, lines.

The presentation of the problem is simplified by the suppression of one of the dimensions. Solutions for the two-dimensional case can be layered to reproduce the three-dimensional distribution, thereby permitting simplification without loss of information.

The use of polar coordinates on the two-dimensional equivalent of eqn. (9-1) yields

$$\int f(x,y) dS = \varphi(\rho, \theta) \quad (9-2)$$

where ρ varies to cover the domain of $f(x,y)$ and θ varies between $\pm \pi/2$. Eqn. (9-2) then becomes the fundamental integral equation to be solved.

If the refractive index field is radially symmetric or if it is independent of one of the coordinates, then the solution of eqn. (9-2) is known and has been extensively used in interferometric studies. For $f(x,y)=f(y)$ only, eqn. (9-2) becomes

$$\varphi(y) = \int_{-L/2}^{L/2} n(y) dx = L n(y) \quad (9-3)$$

and the solution is $n(y) = \varphi(y) L$.

For the radially symmetric case, only one field of view is necessary and eqn. (9-2) becomes

$$\varphi(x) = 2 \int_{r=x}^{\infty} f(r) dy = 2 \int_x^{\infty} \frac{f(r) dr}{(r^2-x^2)^{\frac{1}{2}}} \quad (9-4)$$

which is a form of Abel's integral equation.

The solution of eqn. (9-4) may be obtained by converting the integral into a convolution integral by using appropriate transformations. The solution, $f(r)$, then becomes

$$f(r) = \frac{-1}{\pi} \int_r^{\infty} (x^2-r^2)^{\frac{1}{2}} \frac{d}{dx} \left[\frac{\partial \varphi}{\partial x} \frac{1}{x} \right] dx \quad (9-5)$$

Sweeney uses the definitions of Fourier transforms, a few fundamental transform pairs, the procedure for inverting the Fourier transformed

equivalent of eqn. (9-2) as outlined by Junginger and van Haeringen [15], and an introduction of polar coordinates to the transformed equation to yield

$$f(r, \varphi) = \frac{1}{2\pi^2} \int_{-\pi/2}^{\pi/2} d\theta \left[\frac{\partial \varphi(z, \theta)}{\partial z} * \frac{1}{z} \right] \quad (9-6)$$

where "*" denotes the convolution. Expanding the convolution integral and replacing z with $r \sin(\varphi - \theta)$, the final result for $f(r, \varphi)$ is:

$$f(r, \varphi) = \frac{1}{2\pi^2} \int_{-\pi/2}^{\pi/2} d\theta \int_{-\infty}^{+\infty} \frac{\partial \varphi(\rho, \theta)}{r \sin(\varphi - \theta)} \frac{1}{-\rho} \partial \rho \quad (9-7)$$

This is the basic relationship between the pathlength function and the refractive index field.

Referring to eqn. (9-6), the integral over θ is a linear summation of the contributions for each direction of view. The contribution from each value of θ is equal to the convolution of the derivative of the path length function and, $(1/z)$ with $(1/z)$ evaluated at $z = r \sin(\varphi - \theta)$

When $\rho = r \sin(\varphi - \theta)$, the integrand of eqn. (9-7) becomes singular. This presents no problem since the contributions to the integral near the origin tend to cancel for an odd function (like $1/z$). Thus the integral remains finite.

The integration over ρ in eqn. (9-7) is a Hilbert transform of $\varphi(\rho, \theta)$ and the properties of Hilbert transforms along with the use of discrete data, guarantee the boundness of eqn. (9-7). Both this form of the integration over ρ and Van Houten's [17] modification to it will be called the inside integral in the next section.

A finite number of values of the frequency plane must be determined. One method for their determination uses linear interpolation from adjacent radial lines of a superimposed grid system. Success of this method depends on the accuracy of the interpolation. If the pathlength data is

taken for a sufficiently large number of angular orientations, linear interpolation may be used.

These linearly interpolated frequency plane values ($\phi(\rho, \theta)$) must be convoluted with $1/z$, i.e.

$$[\phi(\rho, \theta) * 1/z] \quad (9-8)$$

with "*" meaning convolution.

Using the following notation of F for obtaining the discrete Fourier transform (DFT) and F^{-1} for obtaining the inverse DFT or IDFT, the remaining steps required to perform the integration over ρ are summarized as follows:

The DFT of the convolution is obtained

$$F[\phi(\rho, \theta) * 1/z] \quad (9-9)$$

followed by the differentiation of this function

$$d(F[\phi(\rho, \theta) * 1/z]) \quad (9-10)$$

Finally the value for the integration over ρ is obtained by taking the IDFT of the preceeding function.

$$F^{-1} [d(F[\phi(\rho, \theta) * 1/z])] \quad (9-11)$$

Van Houten [17] used the linear interpolation approach to obtain the frequency plane values by a computer program designed to calculate the three-dimensional density field from data obtained from holographic interferometry. The frequency plane values for the density field are represented by expanded fringe shift information calculated from the fringe number of specific points on the interferogram. Van Houten modified eqn. (9-7), the basic interferometric equation to the following:

$$f(x_o, y_o) = \frac{-1}{2\pi^2} \int_0^\pi \left[\int_0^{3RMAX} \frac{g(\rho_o + \rho, \varphi) + g(\rho_o - \rho, \varphi) - 2g(\rho_o, \varphi)}{2} d\rho \right. \\ \left. + \frac{2g(\rho_o, \varphi)}{3RMAX} \right] d\varphi \quad (9-12)$$

with $g(\rho, \varphi)$ being the expanded fringe shift information and the integral inside the brackets referred to as the inside integral instead of the integration over ρ .

Van Houten's computer program uses Cote's sixth order method [18] for integrating the first term of the inside integral. He applied a correcting term for the contribution of the integral from 3RMAX to infinity. The sum of these two terms is called the inside integral. If NP is the number of data points for each view, and if K is the number of views, the inside integral must be evaluated $(NP \cdot K)$ times with Van Houten's computer program. Additionally, for each of the NP^2 grid intersections, K interpolations for $G(\rho_o, \varphi_k)$ are required. The subsection of Van Houten's computer program which calculates the value of the inside integral is included in Appendix B. The next section will investigate alternatives for this part of Van Houten's computer program.

X. APPLICATION OF THE FAST FOURIER TRANSFORM

Fast Fourier transform (FFT) methods are simply a more efficient means of obtaining the discrete Fourier transform (DFT). Their increased efficiency is due to the significant reduction in the number of complex mathematical operations required. For a function of N points, normal calculation of the DFT requires nearly N^2 operations while the FFT radix-2 method reduces this to $(N/2) \log_2(N)$ complex multiplications, $(N/2) \log_2(N)$ complex additions, and $(N/2) \log_2(N)$ complex subtractions. As can be seen from Figure 15, for $N=1024$, this results in a computational savings of more than 200 to 1. [19] Higher radix FFT methods further reduce the number of operations required.

Operations usually associated with FFT applications include: (1) computing a spectrogram; (2) computing the convolution of two time series; and (3) computing the correlation of two time series. The second of these operations has been shown to have direct application to the calculation of the value of the inside integral for determining the three-dimensional density field. Reference 20 gives a thorough discussion of the FFT and the required steps for convolution and correlation. These detailed procedures for computing the convolution are included in Appendix C for the following combination of functions: (1) two finite length functions; (2) a finite and an infinite length function using the select-savings method; and (3) a finite and an infinite length function using the overlap-add method.

Two original Fortran programs were devised to apply FFT methods to the calculation of the values of the inside integral. Specifically, alternatives to Mode One operation of Van Houten's computer program for the

asymmetric Gaussian case of $f(z) = (1-y^2) \exp(-2x^2)$ for 65 points from $-1.5 \leq R \leq 1.5$ were investigated. Mode One operation of Van Houten's program requires refractive index information supplied by SUBROUTINE INPUT. Using a finite sample of 65 points with an interval between samples of .046875, Van Houten's program required 1.3388 seconds of computer time just to calculate the value of the inside integral. This time was obtained by using computer library subroutines SETIME and GETIME placed just prior to and immediately after the subsection of Van Houten's computer program which calculates the value of the inside integral.

Van Houten's program also uses a SUBROUTINE COEFF to calculate coefficients used in various parts of the program. MODE1, a modification of Van Houten's program which eliminated the need for SUBROUTINE COEFF by returning its calculations to the main program, is included in Appendix D. This modification includes the essentials of Van Houten's thesis with the following corrections: $C1 = .292857$ instead of .2292857; several divisions by 59.296 were corrected to 57.296; and all plotting directions were deleted due to the storage space limitation of the IBM 360 on-line time sharing capability. This modification followed the work done by Everett [21].

Both FFT method programs used a finite sample of the expanded fringe shift information obtained from Van Houten's computer program. His method for obtaining these frequency plane values followed the linear interpolation approach as described by Sweeney. Sixty-five finite sample points were obtained and they had to be convoluted with the infinite function $1/z$. JONES1 numerically convoluted these functions while JONES2 used the FFT select-savings method to obtain the convolution. Once the convolution was obtained, both programs followed the procedures described in the preceding section, except that FFT methods were used to obtain all

DFT's and IDFT's. The two separate approaches for calculating the convolution served as an internal check that the correct convolution was being obtained. The complete programs are included in Appendix F. along with a listing of the expanded fringe shift information obtained from Van Houten's program and used as frequency plane values for both programs.

The numerical methods used in JONES1 required multiplying the final result by the appropriate weight function, the interval between sampled points of the expanded fringe shift information. JONES2 used the FFT select-savings method to calculate the convolution. The dimension of the $1/R$ vector was chosen to be 512 following Brigham's [20] recommendation as the optimal choice for values of Q between 50 and 99. His table of recommendations for the size of arrays needed for FFT convolution is included in Figure 16. The sample interval for both of these FFT programs was selected to agree with the interval used in Van Houten's program, namely .046875. For $N = 512$, and DR being defined as $2R_{MAX}/N$, an R of 12.0 was required. Using FFT methods to obtain the Fourier coefficients of the convolution also required a weighting function. In the complex multiplication of the normalized Fourier coefficients of the expanded fringe shift information and the $1/R$ vector, the resulting Fourier coefficients incorporated an extra division by N . Instead of a weighting function of DR then, $2R$ was chosen as the appropriate weighting function. When the IDFT of the Fourier coefficients was obtained, the values of the convolution by this FFT method were in exact agreement with the convolution obtained by numerical methods.

The differentiation technique used in JONES1 and JONES2 required an increment between steps of differentiation that was equal to the sample data interval. Thus, the same DR was used for this process.

All FFT calculations in both programs utilized SUBROUTINE CFFT2, an algorithm for computing the mixed radix fast Fourier transform [22]. The complete single precision version of CFFT2 is included in Appendix E. Chosen for its versatility, it contains a detailed and straight-forward usage description at the beginning of the subroutine. Several known Fourier transform pairs were investigated to ensure that CFFT2 was being used correctly. Correct DFT's and IDFT's were easily obtained.

As was previously mentioned, FFT methods involve complex mathematical operations. When using only real functions, as was the case with the expanded fringe shift samples and the $1/z$ function, the frequency plane values could be placed in the real coefficient array of CFFT2 and the other function could be placed in the imaginary coefficient array of the same call to CFFT2. This would result in the significant reduction of time and storage space required to calculate DFT's and IDFT's. This increased efficiency was not utilized in either JONES1 or in JONES2. Instead, both programs are quite inefficient, with redundant storage used for recording and checking each step in the entire process of calculating the value of the inside integral. If one only desired a print-out of the inside integral values, these programs could easily be reduced to four matrices, and possibly to two matrices since both functions were real in this case. Both programs, designed as possible alternatives for Van Houten's subsection that calculated the value of the inside integral, were only written to replace inside integral calculations for Mode One operation. Hence, in addition to condensing these programs into efficient packages, investigation of all other modes of operation is required before a complete integration of FFT methods into Van Houten's program can be achieved.

XI. RESULTS AND RECOMMENDATIONS FOR FFT APPLICATION

The computer time required for just the calculation of the inside integral subsection of Van Houten's program for Mode One operation of the asymmetric Gaussian case took 1.3388 seconds. Although the increased efficiency of FFT methods are significant for large values of N, it was not known if FFT methods would reduce computational time required in this case where N was only 64 sample intervals. Nevertheless, if time had permitted integration of a condensed and efficient form of either JONES1 or JONES2 into Van Houten's program, it was felt that some reduction in computation time would have been achieved.

Both approaches to obtain the convolution, JONES1 using numerical methods and JONES2 using FFT methods, produced convolution values in exact agreement with each other and inside integral values within .002 per cent of each other. A listing of these results side by side to the inside integral values obtained from Van Houten's program is included in Appendix G. There was general agreement between the values of the inside integral as calculated by Van Houten's program compared with those obtained by FFT methods. Near a value of R equal to $\pm .8$ the apparently significant percentage difference between the two methods was misleading since the magnitudes involved were small. However, for values of R near the discontinuity in the density, there was significant disagreement in the values of the inside integral. Further analysis as to the accuracy of the methods involved is required to resolve this problem.

Shifting the expanded fringe shift information from the middle of its array to the beginning of an array whose remaining points were filled with zeros, as suggested by the select-savings method, resulted in the

inside integral values corresponding to the $-1.5 \leq R \leq 1.5$ interval being stored in the output array beginning with the $(N/2 + 1)$ position. In this case, the appropriate values of the inside integral were stored from the 257th through the 321st positions of the output vector. According to the select-savings method (refer to Appendix C.2), the first "Q-2" points of the output vector are meaningless. Q is defined as the number of frequency plane samples used in the calculation of the convolution.

XII. SUMMARY OF RESULTS

An experimental setup was designed and constructed to conduct holographic investigation of a rear-facing step in supersonic flow. Although the double-exposed (frozen) holograms produced did not warrant further analysis of discrepancies of the Chapman-Korst flow model, they were of sufficient quality to demonstrate an application of holography to rear-facing step flow visualization near vibrating equipment such as the supersonic blowdown wind tunnel.

Theoretical investigations of current data reduction techniques for determining the three-dimensional density field from interferometric data led to investigation of the applicability of fast Fourier transform methods to reduce computational time required for determining the inside integration over ρ in the basic interferometric equation. Two programs were devised which calculated the value of the inside integral using FFT methods. Although the convolution was obtained differently for each program, numerically in JONES1 and with FFT's for JONES2, the convolution's were identical. Comparison of these values with those obtained from Van Houten's program lacked close agreement for the $\pm (1.07 - 1.31)$ intervals for R . The difference between these methods requires further analysis as to the accuracy of the methods. Further analysis is also needed to efficiently reduce JONES 1 and JONES2 and to integrate the programs into Van Houten's program for all of its modes of operation.

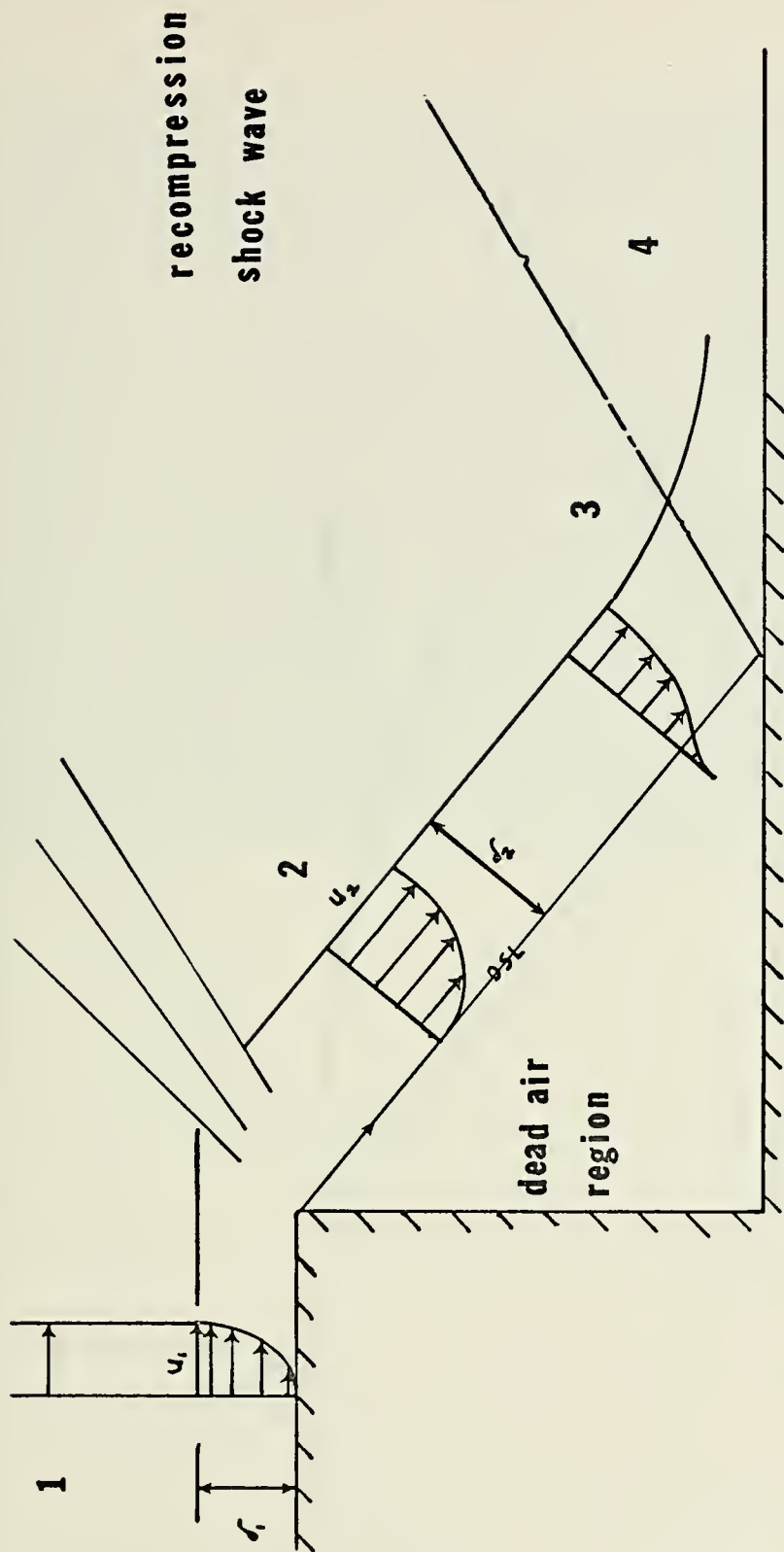


Figure 1. Chapman-Korst Flow Model for Supersonic Base Flow

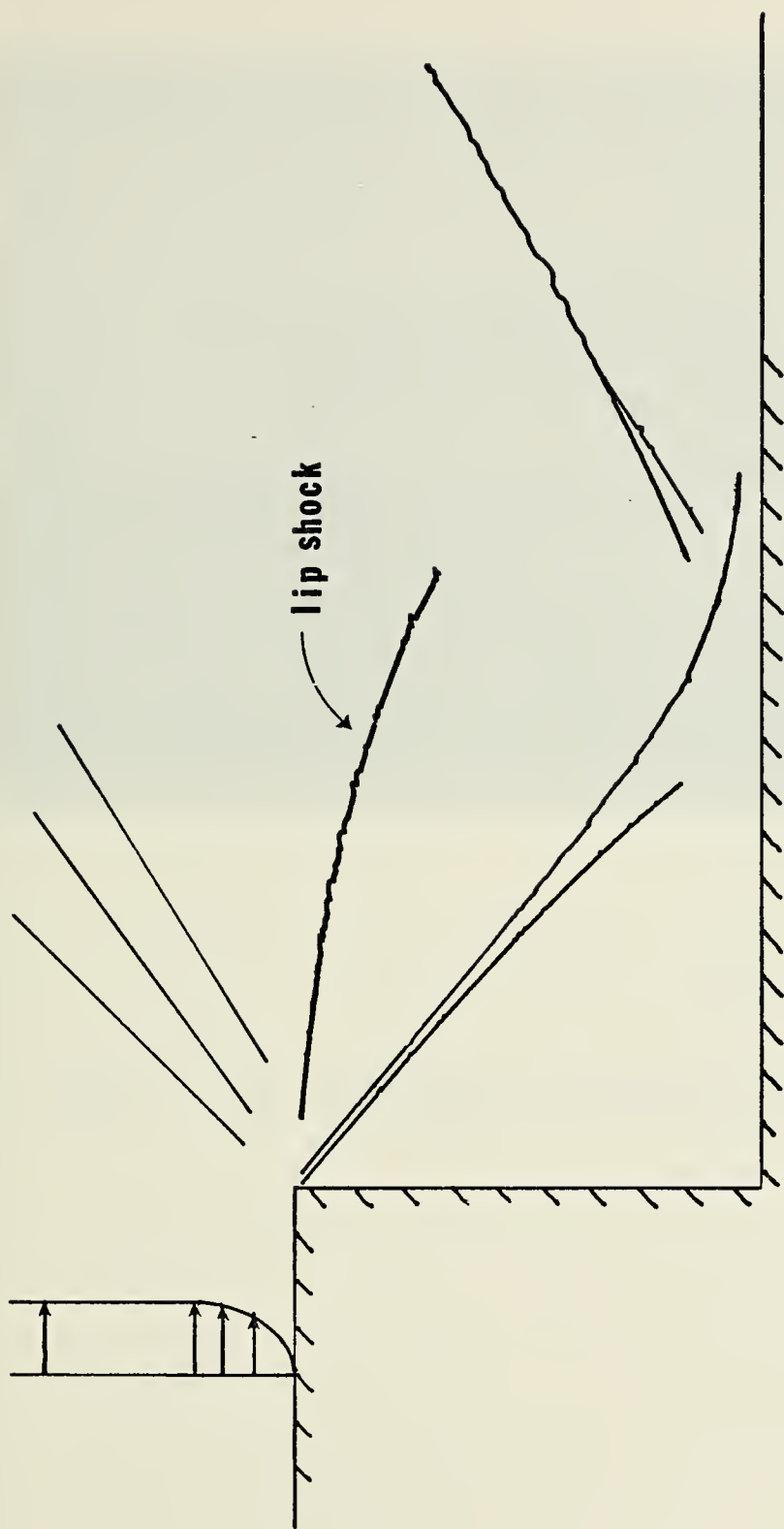


Figure 2. Lip Shock



Figure 3. The Experimental Model of a Rear-Facing Step.



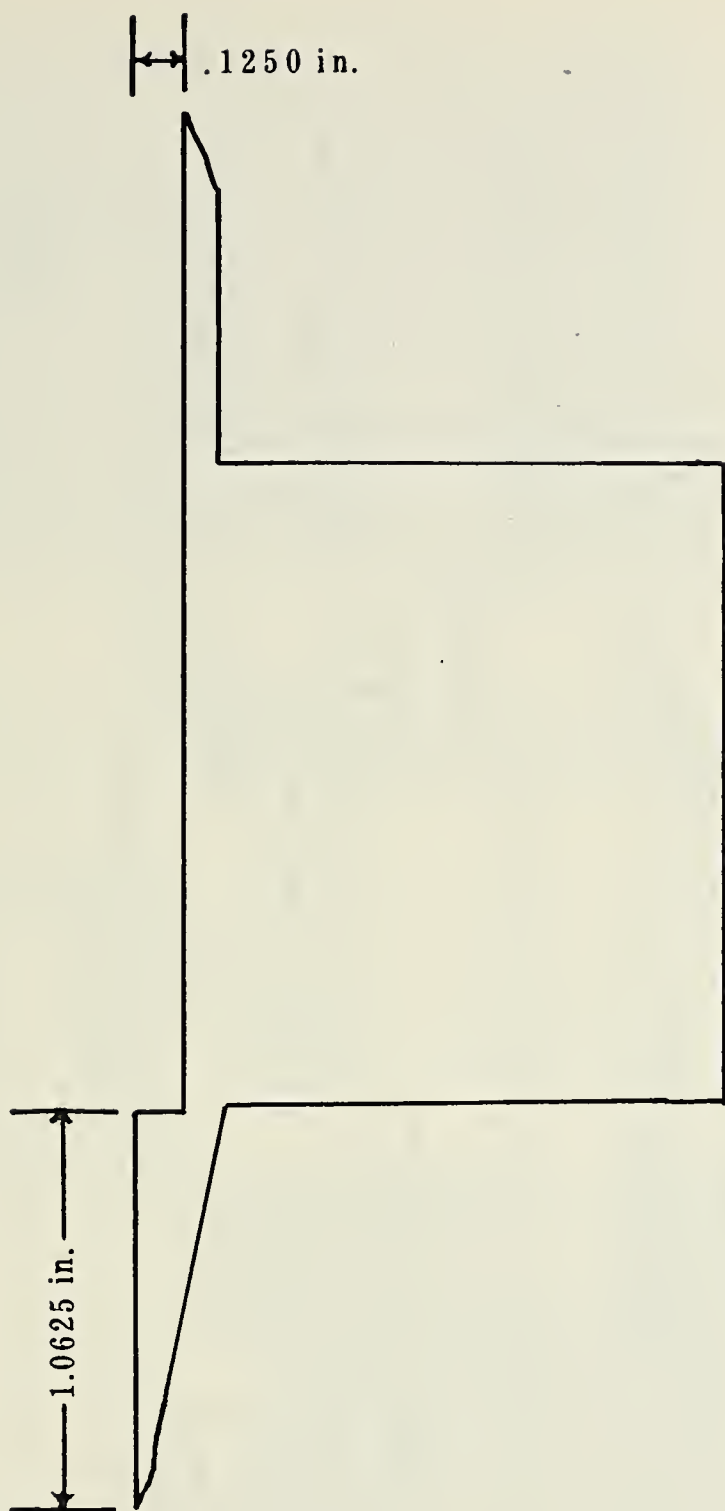


Figure 4. Experimental Model

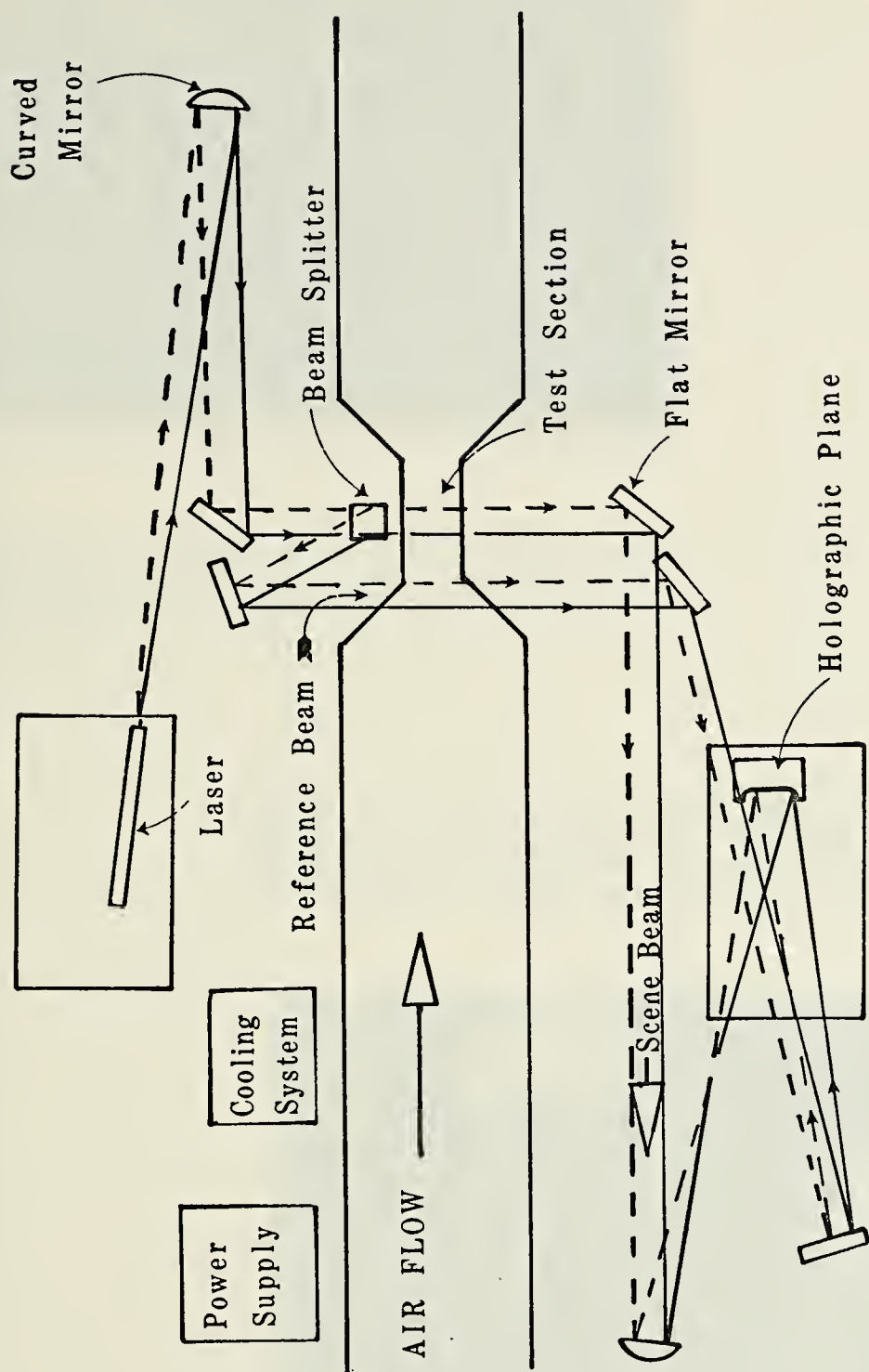


Figure 5. Experimental Setup

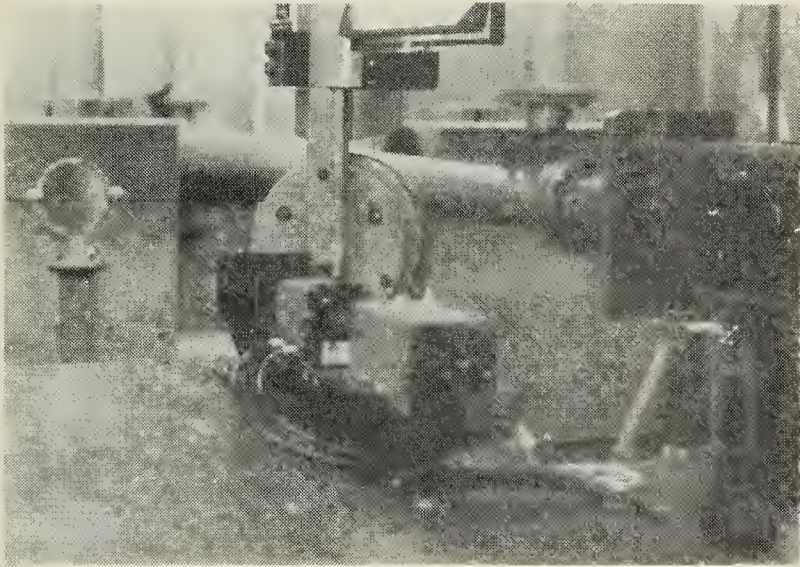
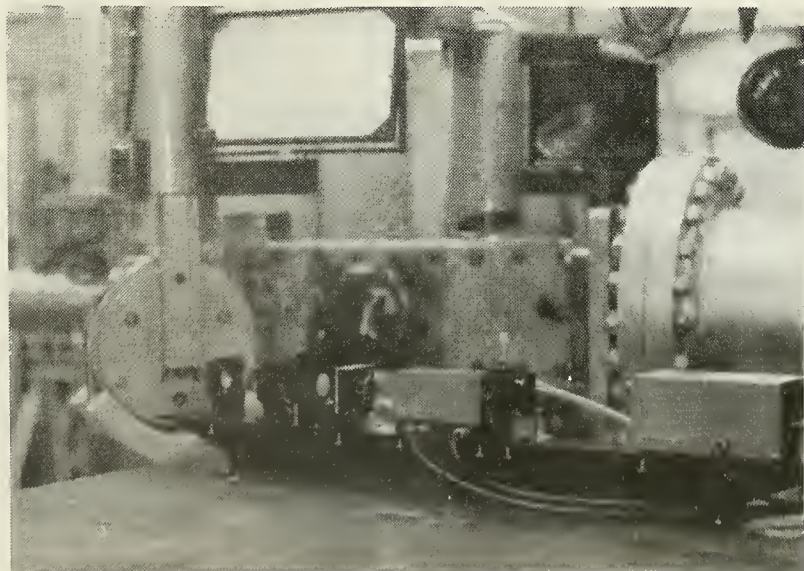


Figure 6. A view of the left side of the the experimental setup showing the laser and the optics system up to the beam splitter.

Figure 7. View of the left side of the test section, also showing the Q-switched laser, the beam splitter, and mirrors which direct the reference beam over the test section.



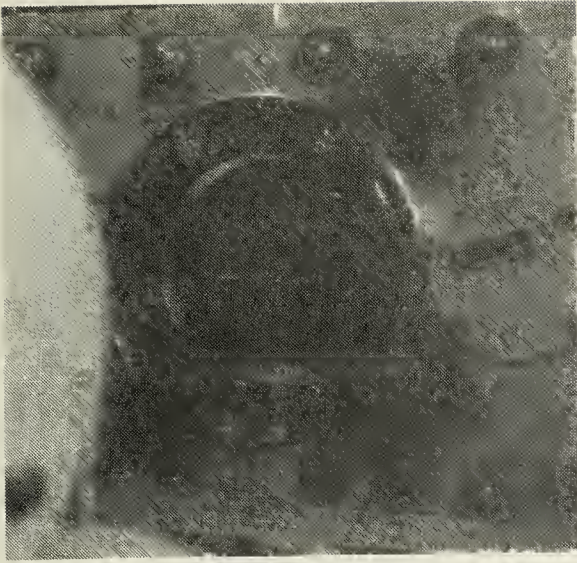
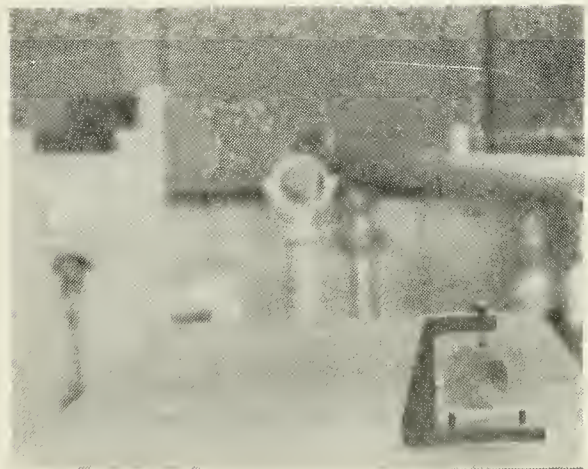


Figure 8.

A view of the right side
of the test section.

Figure 9.

A view of the right side
of the experimental setup
showing the holographic
plane and the final mirrors
for the reference and the
scene beams.



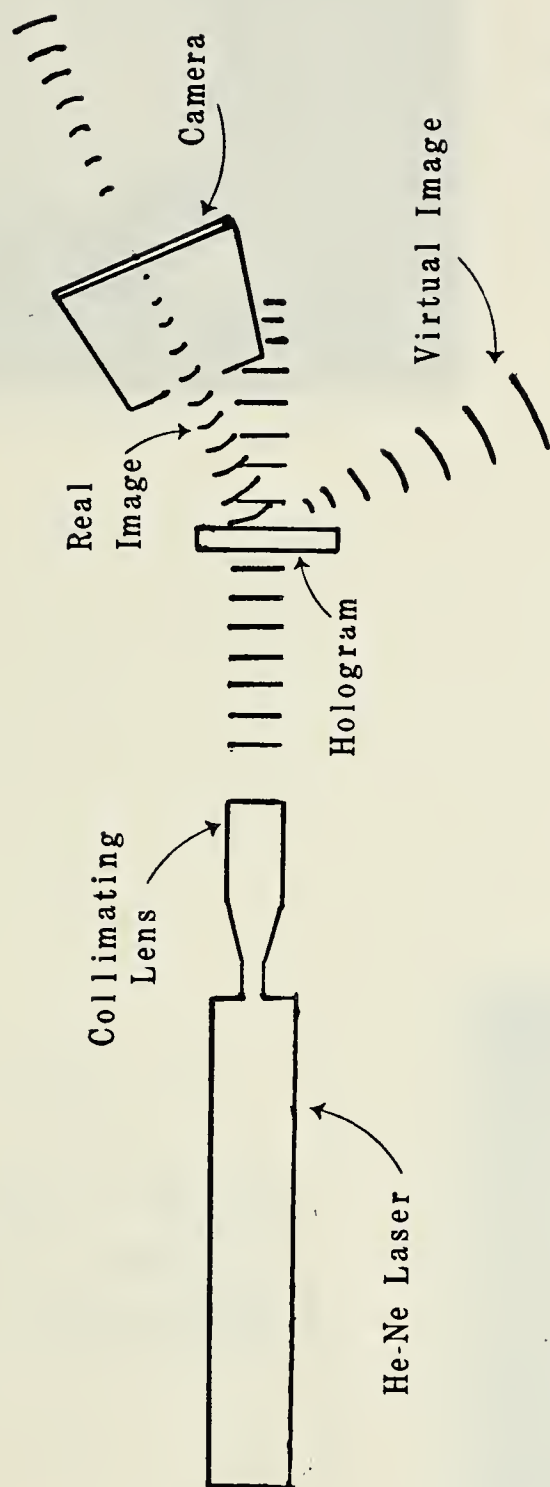


Figure 10. Reconstruction Setup

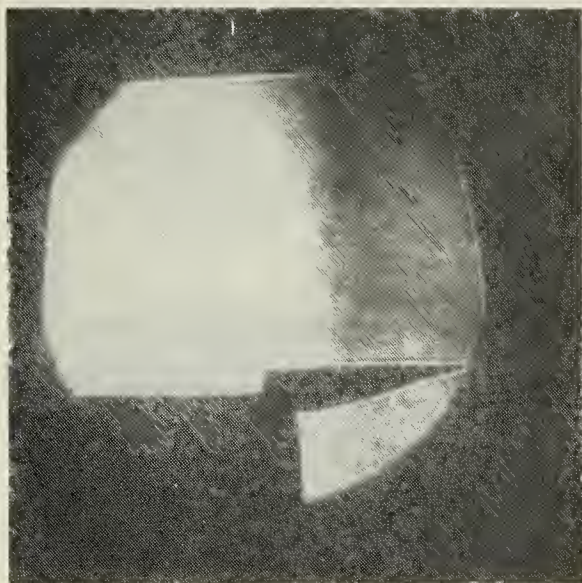


Figure 11.

Photograph of the projected real image of a single-exposed hologram.

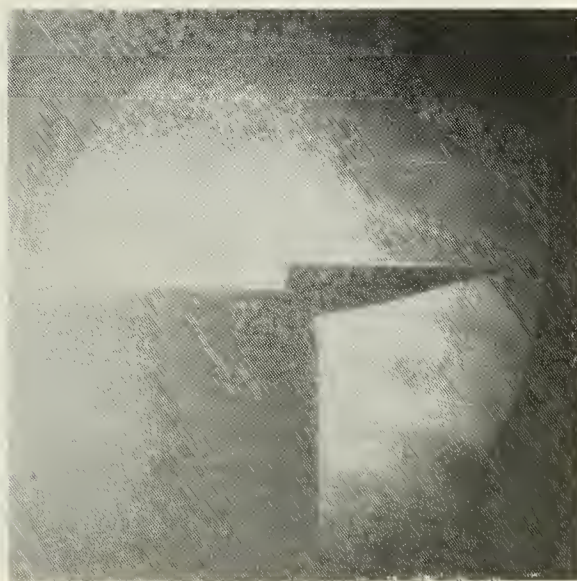


Figure 12.

Photograph of the projected real image of a single-exposed hologram.

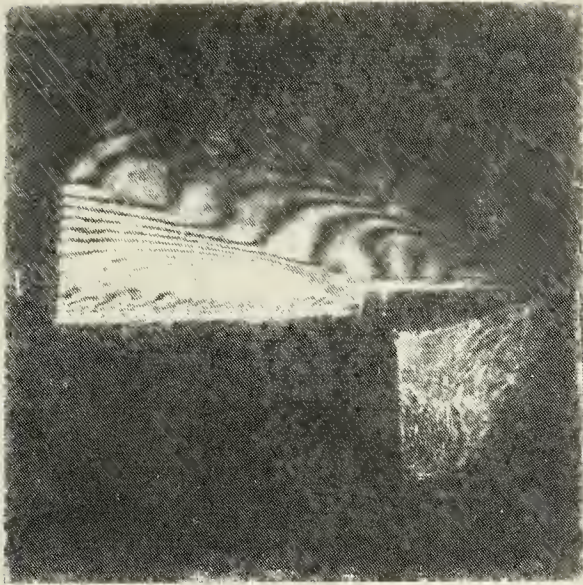
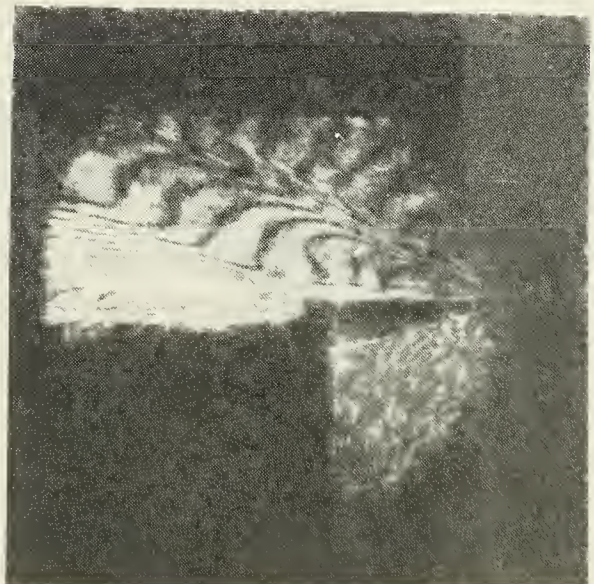


Figure 13.

Photograph of the projected real image of a double-exposed hologram of a rear-facing $1/8$ in. step in Mach 2.8 flow.

Figure 14.

Photograph of the projected real image of a double-exposed hologram of a rear-facing $1/8$ in. step in Mach 2.8 flow.



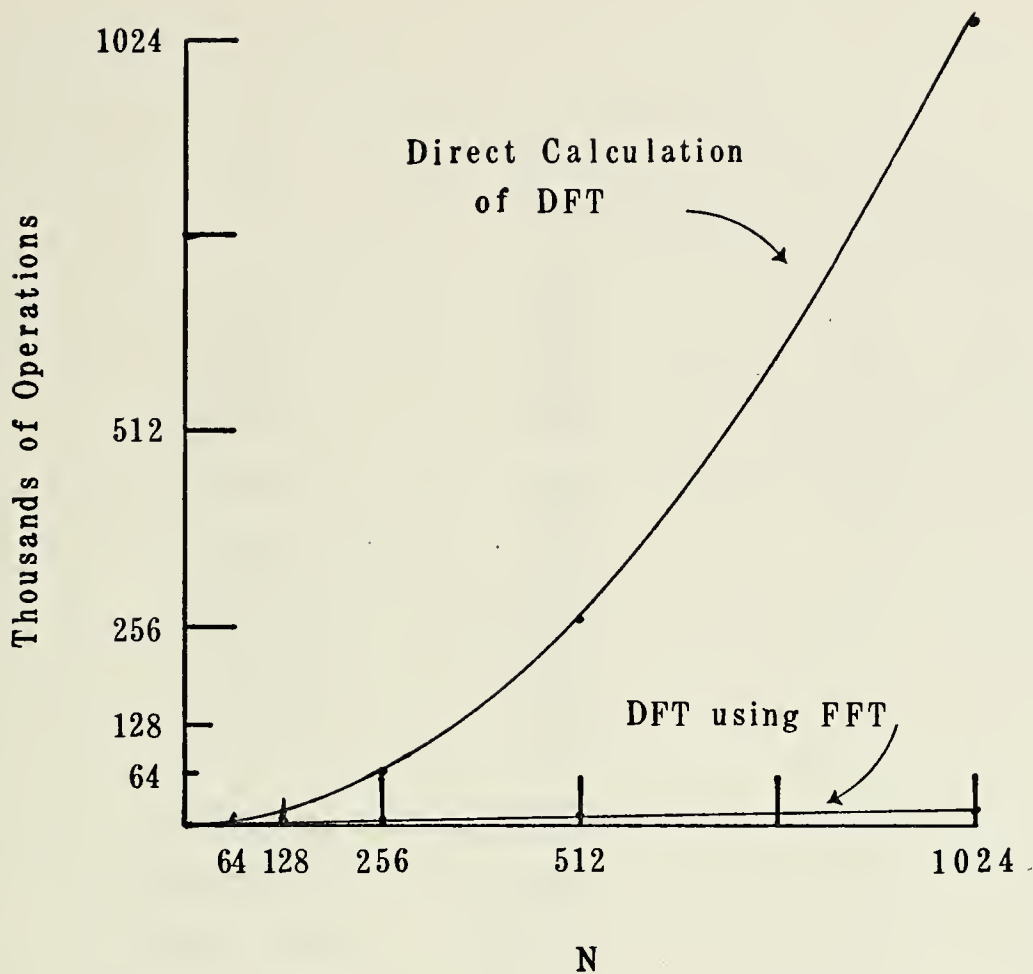


Figure 15. The Number of Operations Required to Compute the Discrete Fourier Transform by Direct Calculation Compared with Using the FFT Algorithm.

Q	N	γ
10	32	5
11-19	64	6
20-29	128	7
30-49	256	8
50-99	512	9
100-199	1024	10
200-299	2048	11
300-599	4096	12
600-999	8192	13
1000-1999	16384	14
2000-3999	32768	15

Optimum Value of N for FFT Convolution.

FIGURE 16.

APPENDIX A. DETAILED EXPERIMENTAL PROCEDURES

I. ALIGNMENT OF SYSTEM:

- a) Turn on cooling system and warm up power supply.
- b) Check internal alignment of laser with autocollimator.
- c) Insert 2.5 mm orifice inside laser cavity in order to eliminate higher order transverse mode emission.
- d) After ensuring all endangered personnel are wearing eye protectors, fire the Q-switch laser to burn a spot on underexposed (black) film.
- e) Make a needle hole in the center of the burn spot and fire the laser again to make a burn spot on another fixed piece of underexposed film. Always check for personnel wearing eye protectors prior to firing the Q-switch laser.
- f) Align a 15 mW CW laser beam through the 2.5 mm orifice and through the pin holes in the two pieces of film by using a flat mirror.
- g) Elevate table so that the laser beam hits the first mirror in the optics system in its center. Ensure that the focal point of the diffusing lens is located at the focal point of the parabolic mirror in order to obtain a collimated beam entering the optics system.
- h) Align optics system, ensuring test section and holographic plane are properly illuminated.
- i) Adjust the location of the holographic plane to ensure that the subject image is in focus in the diverging part of the scene beam.
- j) Adjust the final flat mirror in the reference beam in order to make sure path lengths of the two beams are within one-half inch of each other.

k) Remove CW laser and alignment mirror as well as remaining alignment pinholes.

1) Ready to fire.

II. EXPOSURE OF HOLOGRAPHIC PLATES:

a) Single Pulse (Exposure):

1) Insert plate in holder underneath the black drape.

2) Assistant charges the power supply and notifies experimenter when ready to fire.

3) Experimenter lifts the drape while simultaneously calling to fire the laser, and replaces the drape immediately after observing lamp flash of the Q-switch laser.

4) Remove the exposed holographic plate to a labeled film box while still under the drape to eliminate further exposure.

5) Hologram is ready for development.

b) Double-Pulse (Exposure):

1) Repeat steps II.a.1-3. Wear sound attenuators.

2) Open air supply and create desired flow in the test section.
(Mach 2.8 flow in this experiment)

3) Repeat steps II.a.2-5. Assistant shuts off air supply after firing laser.

APPENDIX B. INSIDE INTEGRAL SUBSECTION OF VAN HOUTEN'S COMPUTER PROGRAM

See Appendix E right hand count labeled EVE02460-2840 for location of this subsection in Van Houten's program.

```

*****CALCULATE VALUE OF INSIDE INTEGRAL *****
DC 43 I=1,NT
DC 43 J=1,NP
M=NPL+J
BD(1)=0.
DO 39 K=1,MAX
MKP=M+K
MKM=M-K
IF(MKP.GT.NPP) MKP=NPP
IF(MKM.LT.1) MKM=1
K1=K**2
39 BC(K+1)=(BB(MKP,I)+BB(MKM,I))-2.*BB(M,I)/(FLOAT(K1)*DR)
VAL=0.
K1=1
40 K2=K1+6
IF(K2.GT.MAX) GO TO 41
*****SIXTH ORDER QUADATURE FORMULA*****
VAL=VAL+C1*(BD(K1)+BD(K2))+C2*(BD(K1+1)+BD(K2-1))+C3*(BD(K1+2)+BD(K2-2))+C4*BD(K1+3)
K1=K2
GO TO 40
41 SUM=0.
*****CONTRIBUTION OF LAST TERM*****
DO 42 K=K1,MAX
SUM=SUM+BD(K)+BD(K+1)
42 SUM=COTES PLUS LAST TERMS PLUS INTEGRATION FROM 2 RMAX TO INFINITY
43 B(J,I)=VAL+SUM/2.-.666667*BB(M,I)/RMAX
IF(KSYM.LT.99) GO TO 48
*****03370
*****03390
*****03400
*****03410
*****03420
*****03430
*****03440
*****03450
*****03460
*****03470
*****03480
*****03490
*****03500
*****03510
*****03520
*****03530
*****03540
*****03550
*****03560
*****03570
*****03580
*****03590
*****03600
*****03610
*****03620
*****03630
*****03640
*****03650

```


APPENDIX C. FFT CONVOLUTION PROCEDURES

C.1 COMPUTATION PROCEDURE FOR FFT CONVOLUTION OF FINITE-LENGTH FUNCTIONS.

1. Let $x(t)$ and $h(t)$ be finite-length functions shifted from the origin by a and b , respectively.

2. Shift $x(t)$ and $h(t)$ to the origin and sample:

$$x(k) = x(KT + a) \quad k = 0, 1, \dots, P - 1$$

$$h(k) = h(KT + b) \quad k = 0, 1, \dots, Q - 1$$

3. Choose N to satisfy the relationships:

$$N \geq P + Q - 1$$

$$N = 2^m \quad \text{integer valued}$$

where P is the number of samples defining $x(t)$ and Q is the number of samples defining $h(t)$.

4. Augment with zeros the sampled functions of step (2).

$$x(k) = 0 \quad k = P, P + 1, \dots, N - 1$$

$$h(k) = 0 \quad k = Q, Q + 1, \dots, N - 1$$

5. Compute the discrete transform of $x(k)$ and $h(k)$.

$$X(n) = \sum_{k=0}^{N-1} x(k) \exp(-j2\pi nk/N)$$

$$H(n) = \sum_{k=0}^{N-1} h(k) \exp(-j2\pi nk/N)$$

6. Compute the product:

$$Y(n) = X(n)H(n)$$

7. Compute the inverse discrete transform using the forward transform:

$$y(k) = \sum_{n=0}^{N-1} \frac{1}{N} Y^*(n) \exp(-j2\pi nk/N)$$

C.2 COMPUTATION PROCEDURE FOR FFT CONVOLUTION: SELECT-SAVINGS METHOD:

1. Let Q be the number of samples representing $h(t)$.
2. Choose N according to the table in Figure 16.
3. Form the sampled periodic function $h(k)$.

$$\begin{aligned} h(k) &= h(kT) & k &= 0, 1, \dots, Q - 1 \\ &= 0 & k &= Q, Q + 1, \dots, N - 1 \end{aligned}$$

4. Compute the discrete Fourier transform of $h(k)$

$$H(n) = \sum_{k=0}^{N-1} h(k) \exp(-j2\pi nk/N)$$

5. Form the sampled periodic function:

$$x_1(k) = x(kT) \quad k = 0, 1, \dots, N - 1$$

6. Compute the discrete Fourier transform of $x_1(k)$.

$$X_1(n) = \sum_{k=0}^{N-1} x_1(k) \exp(-j2\pi nk/N)$$

7. Compute the product:

$$Y_1(n) = X_1(n)H(n)$$

8. Compute the inverse discrete transform of $Y_1(n)$.

$$y_1(k) = \sum_{n=0}^{N-1} \frac{1}{N} Y_1(n) \exp(-j2\pi nk/N)$$

9. Delete samples $y_1(0), y_1(1), \dots, y_1(Q - 2)$, and save the remaining samples.

10. Repeat steps 5 to 9 until all sections are computed.

11. Combine the sectioned results by the relationships:

$$\begin{aligned} y(k) &\text{ undefined} & k &= 0, 1, \dots, Q - 2 \\ y(k) &= y_1(k) & k &= Q - 1, Q, \dots, N - 1 \\ y(k+N) &= y_2(k+Q-1) & k &= 0, 1, \dots, N - Q \\ y(k+2N) &= y_3(k+Q-1) & k &= 0, 1, \dots, N - Q \end{aligned}$$

C.3 COMPUTATION PROCEDURE FOR FFT CONVOLUTION: OVERLAP-ADD METHOD.

1. Let Q be the number of samples representing $h(t)$.
2. Choose N according to the table in Figure 16.
3. Form the sampled periodic function $h(k)$:

$$\begin{aligned} h(k) &= h(kT) & k &= 0, 1, \dots, Q - 1 \\ &= 0 & k &= Q, Q + 1, \dots, N - 1 \end{aligned}$$

4. Compute the discrete Fourier transform of $h(k)$.

$$H(n) = \sum_{k=0}^{N-1} h(k) \exp(-j2\pi nk/N)$$

5. Form the sampled periodic function:

$$\begin{aligned} x_1(k) &= x(kT) & k &= 0, 1, \dots, N - Q \\ &= 0 & k &= N - Q + 1, \dots, N - 1 \end{aligned}$$

6. Compute the discrete Fourier transform of $x_1(k)$.

$$X_1(n) = \sum_{k=0}^{N-1} x_1(k) \exp(-j2\pi nk/N)$$

7. Compute the product:

$$Y_1(n) = X_1(n)H(n)$$

8. Compute the inverse discrete transform of $Y_1(n)$.

$$y_1(k) = \sum_{n=0}^{N-1} \frac{1}{N} Y_1(n) \exp(-j2\pi nk/N)$$

9. Repeat steps 5-8 until all sections are computed.
10. Combine the sectioned results by the relationships:

$$\begin{aligned} y(k) &= y_1(k) & k &= 0, 1, \dots, N - Q \\ y(k+N-Q+1) &= y_1(k+N-Q+1) + y_2(k) & k &= 0, 1, \dots, N - Q \\ y(k+2(N-Q+1)) &= y_2(k+N-Q+1) + y_3(k) & k &= 0, 1, \dots, N - Q \\ &\cdot \\ &\cdot \\ &\cdot \end{aligned}$$

APPENDIX D. SUBROUTINE CFFT2

```

.....
SUBROUTINE CFFT2      (CATEGORY E2)
PURPOSE
    TO COMPUTE THE COMPLEX FOURIER TRANSFORM OR INVERSE IN PLACE
    USING THE MIXED-RADIX FAST FOURIER TRANSFORM ALGORITHM. WITHIN
    CERTAIN LIMITATIONS, DISCUSSED BELOW, AN ARBITRARY NUMBER OF DATA
    POINTS MAY BE PROCESSED. SEE ROUTINE RFFT2 TO PROCESS REAL DATA
    IF THE NUMBER OF DATA POINTS IS EVEN.
USAGE
    CALL CFFT2 (A, B, NTOT, N, NSPAN, ISN)
DESCRIPTION OF PARAMETERS
    A - REAL*4 ARRAY HOLDING THE CONSECUTIVELY STORED REAL COM-
        PONENTS OF DATA (WHEN IABS(ISN) = 1) OR A COMPLEX*8
        ARRAY HOLDING DATA (WHEN IABS(ISN) = 2). AT EXIT FROM
        CFFT2, A WILL HOLD THE REAL COMPONENTS OF THE RESULTING
        REAL*4 FOURIER COEFFICIENTS WHEN IABS(ISN)=1, OR THE
        COMPLEX*8 FOURIER COEFFICIENTS, WHEN IABS(ISN) = 2.
        SEE DESCRIPTION OF 'ISN' BELOW.
    B - WHEN IABS(ISN)=1, B IS A REAL*4 ARRAY HOLDING THE CONSE-
        CUTIVELY STORED IMAGINARY COMPONENTS OF DATA. AT EXIT
        FROM CFFT2 IT WILL CONTAIN THE IMAGINARY COMPONENTS OF
        THE FOURIER COEFFICIENTS. WHEN USING COMPLEX*8 DATA
        (WHEN IABS(ISN)=2) ALWAYS USE 'A(2)', INSTEAD OF 'B'. IN
        THE CALL STATEMENT, SINCE 'A' CONTAINS BOTH THE REAL AND
        IMAGINARY COMPONENTS OF DATA. SEE 'ISN' BELOW.
    NTOT - TOTAL NUMBER OF COMPLEX DATA VALUES INVOLVED. FCR A
        SINGLE-VARIABLE ANALYSIS, NTOT = N. NSPAN = (NUMBER
        OF COMPLEX DATA VALUES). FOR A TRI-VARIATE ANALYSIS
        OF A(N1,N2,N3), AND B(N1,N2,N3), WHERE IABS(ISN) = 1,
        OR COMPLEX A(N1,N2,N3), WHERE IABS(ISN) = 2, NTOT
        WOULD BE THE PRODUCT, N1*N2*N3. (INTEGER*4)
        SEE "EXAMPLES" BELOW.

```

CC

CFFT0430
CFFT0440
CFFT0450
CFFT0460
CFFT0470
CFFT0480
CFFT0490
CFFT0500
CFFT0510
CFFT0520
CFFT0530
CFFT0540
CFFT0550
CFFT0560
CFFT0570
CFFT0580
CFFT0590
CFFT0600
CFFT0610
CFFT0620
CFFT0630
CFFT0640
CFFT0650
CFFT0660
CFFT0670
CFFT0680
CFFT0690
CFFT0700
CFFT0710
CFFT0720
CFFT0730
CFFT0740
CFFT0750
CFFT0760
CFFT0770
CFFT0780
CFFT0790
CFFT0800
CFFT0810
CFFT0820
CFFT0830
CFFT0840
CFFT0850
CFFT0860
CFFT0870
CFFT0880
CFFT0890
CFFT0900

N - DIMENSION OF CURRENT VARIABLE. IDENTICAL TO NTOT AND NSPAN AND THE NUMBER OF COMPLEX DATA VALUES IN SINGLE VARIABLE CASE. SEE "EXAMPLES" BELOW FOR CASES OF HIGHER DIMENSIONALITY. (INTEGER*4)

NSPAN - NSPAN/N IS THE SPACING OF CONSECUTIVE DATA VALUES WHEN INDEXING CURRENT VARIABLE. IT IS IDENTICAL TO NTOT AND N AND NC. CF COMPLEX DATA POINTS IN THE SINGLE-VARIABLE CASE. SEE "EXAMPLES" BELOW FOR MULTI-VARIABLE CASES. (INTEGER*4)

ISN - AN INTEGER*4 CONTROL VARIABLE BY WHICH USER SPECIFIES BOTH THE STORAGE MODE OF HIS DATA (AND RESULTING FOURIER COEFFICIENTS) AND WHETHER HE WANTS THE DISCRETE FOURIER TRANSFORM (DFT) OR THE INVERSE DISCRETE FOURIER TRANSFORM (IDFT).

IF ISN IS NEGATIVE THE DFT IS OBTAINED; IF ISN IS POSITIVE THE IDFT IS OBTAINED. IF ISN IS +1 OR -1, THE REAL COMPONENTS OF THE DATA SHOULD BE IN THE REAL*4 ARRAY 'A' AND THE IMAGINARY COMPONENTS IN THE REAL*4 ARRAY 'B'. BOTH OF WHICH SHOULD BE DIMENSIONED AT LEAST 'NTOT'. IF ISN IS +2 OR -2, THE COMPLEX DATA SHOULD BE STORED IN THE COMPLEX*8 ARRAY 'A' (AT LEAST NTOT IN LENGTH) AND THE SECOND ARGUMENT IN THE CALLING LIST SHOULD BE 'A(2)'.
H

REMARKS

DEFINITIONS: THE DISCRETE FOURIER TRANSFORM (DFT) OF $X(J)$ FOR $J=1(1)N$, IS $1/N$ TIMES THE SERIES GIVEN BY:

$$Y(K) = \sum_{J=1}^N X(J) * \exp(-2.*PI * I * J * K / N),$$

FOR $K = 1(1)N$.

(HERE "I" STANDS FOR $\sqrt{-1}$) AND $PI = 3.141593$.)

THE INVERSE DISCRETE FOURIER TRANSFORM (IDFT) OF $Y(J)$, $J=1,N$ IS THE SUMMATION FOR $K = 1(1)N$, OF THE TERMS,

$$Y(K) * \exp(2.*PI * I * J * K / N).$$

IMPORTANT NOTE: CFFT2 RETURNS THE UNNORMALIZED DFT WHEN ISN .LT. 0. THE RESULT VECTOR MUST BE DIVIDED BY N (NUMBER OF COMPLEX DATA POINTS) TO PRODUCE THE NORMALIZED DFT.

NOTES ON NUMBER OF DATA POINTS:

CC

CFFT1870
 CFFT1880
 CFFT1890
 CFFT1900
 CFFT1910
 CFFT1920
 CFFT1930
 CFFT1940
 CFFT1950
 CFFT1960
 CFFT1970
 CFFT1980
 CFFT1990
 CFFT2000
 CFFT2010
 CFFT2020
 CFFT2030
 CFFT2040
 CFFT2050
 CFFT2060
 CFFT2070
 CFFT2080
 CFFT2090
 CFFT2100
 CFFT2110
 CFFT2120
 CFFT2130
 CFFT2140
 CFFT2150
 CFFT2160
 CFFT2170
 CFFT2180
 CFFT2190
 CFFT2200
 CFFT2210
 CFFT2220
 CFFT2230
 CFFT2240
 CFFT2250
 CFFT2260
 CFFT2270
 CFFT2280
 CFFT2290
 CFFT2300
 CFFT2310
 CFFT2320
 CFFT2330
 CFFT2340

```

C      S72 = SIN(S72)
      S120 = .8660254D0
      IF (ISN .GE. 0) GO TO 10
      S72 = -S72
      S120 = -S120
      RAD = -RAD
      INC = -INC

C      10 NT = INC * NTOT
      KS = INC * NSPAN
      KSPAN = KS
      NN = NT - INC
      JC = KS/NN
      RADF = RAD * FLOAT(JC) * .5
      I = 0
      JF = 0

      DETERMINE FACTORS OF N

      M = 0
      K = N
      GC TO 20

C      15 M = M + 1
      NFAC(M) = 4
      K = K/16

C      20 IF (K - (K/16) * 16 .EQ. 0) GO TO 15
      J = 3
      JJ = 9
      GC TO 30

C      25 M = M + 1
      NFAC(M) = J
      K = K/JJ

C      30 IF (MOD(K,JJ) .EQ. 0) GO TO 25
      J = J + 2
      JJ = J*2
      IF (JJ .LE. K) GO TO 30
      IF (K .GT. 4) GO TO 40
      KT = M
      NFAC(M+1) = K
      IF (K .NE. 1) M = M+1
      GC TO 80

C      40 IF (K - (K/4)*4 .NE. 0) GO TO 50
  
```


CFFT2350
 CFFT2360
 CFFT2370
 CFFT2380
 CFFT2390
 CFFT2400
 CFFT2410
 CFFT2420
 CFFT2430
 CFFT2440
 CFFT2450
 CFFT2460
 CFFT2470
 CFFT2480
 CFFT2490
 CFFT2500
 CFFT2510
 CFFT2520
 CFFT2530
 CFFT2540
 CFFT2550
 CFFT2560
 CFFT2570
 CFFT2580
 CFFT2590
 CFFT2600
 CFFT2610
 CFFT2620
 CFFT2630
 CFFT2640
 CFFT2650
 CFFT2660
 CFFT2670
 CFFT2680
 CFFT2690
 CFFT2700
 CFFT2710
 CFFT2720
 CFFT2730
 CFFT2740
 CFFT2750
 CFFT2760
 CFFT2770
 CFFT2780
 CFFT2790
 CFFT2800
 CFFT2810
 CFFT2820

```

      M = M + 1
      NFAC(M) = 2
      K = K/4
    50  KT = M
       J = 2
    60  IF (MOD(K,J) .NE. 0) GO TO 70
       M = M+1
       NFAC(M) = J
       K = K/J
    70  J = ((J+1)/2)*2 + 1
       IF (J .LE. K) GO TO 60
    80  IF (KT .EQ. 0) GO TO 100
       J = KT
    90  M = M+1
       NFAC(M) = NFAC(J)
       J = J-1
       IF (J .NE. 0) GO TO 90
      C      COMPUTE FOURIER TRANSFORM
    100 SD = RADF/ FLGAT(KSPAN)
       CC = 2.0 * SIN(SD)**2
       SD = SIN(SD+SD)
       KK = 1
       I = I + 1
       IF (NFAC(I) .NE. 2) GO TO 400
      C      TRANSFORM FOR FACTOR OF 2 (INCLUDING RTATION FACTOR)
      C      KSPAN = KSPAN/2
      C      K1 = KSPAN + 2
    210 K2 = KK + KSPAN
       AK = A(K2)
       BK = B(K2)
       A(K2) = A(KK) - AK
       B(K2) = B(KK) - BK
       A(KK) = A(KK) + AK
       B(KK) = B(KK) + BK
      C      KK = K2 + KSPAN
      C      IF (KK .LE. NN) GO TO 210
      C      KK = KK - NN
  
```



```

C 220 C1 = 1.0 -CD
      S1 = SD
      K2 = KK + KSPAN
      AK = A(KK) - A(K2)
      BK = B(KK) - B(K2)
      A(KK) = A(KK) + A(K2)
      B(KK) = B(KK) + B(K2)
      A(K2) = C1 * AK - S1 * BK
      B(K2) = S1 * AK + C1 * BK
      KK = K2 + KSPAN
      IF (KK.LT.NT) GO TO 230
      K2 = KK - NT
      C1 = -C1
      KK = K1 - K2
      IF (KK.GT.K2) GO TO 230
      S1 = C1 - (CD * C1 - CD * S1) + S1
      C1 = 0.5/(AK**2 + S1**2) + 0.5
      S1 = C1 * S1
      C1 = C1 * AK
      KK = KK + JC
      IF (KK.LT.K2) GO TO 230
      K1 = K1 + INC + INC
      KK = (K1 - KSPAN)/2 + JC
      IF (KK.LE.JC+JC) GO TO 220
      GC TO 100
      TRANSFORM FOR FACTOR OF 3
C 320 K1 = KK + KSPAN
      K2 = K1 + KSPAN
      AK = A(KK)
      BK = B(KK)
      AJ = A(K1) + A(K2)
      BJ = B(K1) + B(K2)
      A(KK) = AK + AJ
      B(KK) = BK + BJ
      AK = -0.5 * AJ + AK
      BK = -0.5 * BJ + BK
      AJ = (A(K1) - A(K2)) * S120
      BJ = (B(K1) - B(K2)) * S120

```

```

CFFFT2830
CFFFT2840
CFFFT2850
CFFFT2860
CFFFT2870
CFFFT2880
CFFFT2890
CFFFT2900
CFFFT2910
CFFFT2920
CFFFT2930
CFFFT2940
CFFFT2950
CFFFT2960
CFFFT2970
CFFFT2980
CFFFT2990
CFFFT3000
CFFFT3010
CFFFT3020
CFFFT3030
CFFFT3040
CFFFT3050
CFFFT3060
CFFFT3070
CFFFT3080
CFFFT3090
CFFFT3100
CFFFT3110
CFFFT3120
CFFFT3130
CFFFT3140
CFFFT3150
CFFFT3160
CFFFT3170
CFFFT3180
CFFFT3190
CFFFT3200
CFFFT3210
CFFFT3220
CFFFT3230
CFFFT3240
CFFFT3250
CFFFT3260
CFFFT3270
CFFFT3280
CFFFT3290
CFFFT3300

```



```

C      A(K1) = AK - BJ
C      B(K1) = BK + AJ
C      A(K2) = AK + BJ
C      B(K2) = BK - AJ
C      KK = K2 + KSPAN
C      IF (KK.LT.NN) GO TO 320
C      IF (KK.LE.NN) KSPAN) GO TO 320
C      GC TO 700
C
C      TRANSFORM FOR FACTOR OF 4
C
C      400 IF (NFAC(I).NE.4) GO TO 600
C      KSPNN = KSPAN
C      KSPAN = KSPAN/4
C
C      410 C1 = 1.0
C      S1 = 0.0
C
C      420 K1 = KK + KSPAN
C      K2 = K1 + KSPAN
C      K3 = K2 + KSPAN
C      AKP = A(KK) + A(K2)
C      AKM = A(KK) - A(K2)
C      AJP = A(K1) + A(K3)
C      AJM = A(K1) - A(K3)
C      A(KK) = AKP + AJP
C      AJP = AKP - AJP
C
C      BKP = B(KK) + B(K2)
C      BKM = B(KK) - B(K2)
C      BJP = B(K1) + B(K3)
C      BJM = B(K1) - B(K3)
C      B(KK) = BKP + BJP
C      BJP = BKP - BJP
C
C      IF (ISN.LT.0) GO TO 450
C      AKP = AKM - BJM
C      AKM = AKM + BJM
C
C      BKP = BKM + AJM
C      BKM = BKM - AJM
C      IF (S1.EQ.0.0) GO TO 460
C
C      430 A(K1) = AKP*C1 - BKP*S1
C      B(K1) = AKP*S1 + BKP*C1
C
C      A(K2) = AJP*C2 - BJP*S2

```

```

CFFT33310
CFFT33320
CFFT33330
CFFT33340
CFFT33350
CFFT33360
CFFT33370
CFFT33380
CFFT33390
CFFT33400
CFFT33410
CFFT33420
CFFT33430
CFFT33440
CFFT33450
CFFT33460
CFFT33470
CFFT33480
CFFT33490
CFFT33500
CFFT33510
CFFT33520
CFFT33530
CFFT33540
CFFT33550
CFFT33560
CFFT33570
CFFT33580
CFFT33590
CFFT33600
CFFT33610
CFFT33620
CFFT33630
CFFT33640
CFFT33650
CFFT33660
CFFT33670
CFFT33680
CFFT33690
CFFT33700
CFFT33710
CFFT33720
CFFT33730
CFFT33740
CFFT33750
CFFT33760
CFFT33770
CFFT33780

```



```

C      B(K2) = AJP*S2 + BJP*C2
C      A(K3) = AKM*C3 - BKM*S3
C      B(K3) = AKM*S3 + BKM*C3
C      KK = K3 + KSPAN
C      IF (KK.LE. NT) GO TO 420
C      440 G2 = C1 - (CD*C1 + SD*S1)
C      S1 = (SD*C1 - CD*S1) + S1
C      C1 = 0.5/(C2**2 + S1**2) + 0.5
C      S1 = C1*S1
C      C2 = C1**2 - S1**2
C      S2 = 2.0*C1*S1
C      C3 = C2**2 - S2**2
C      S3 = C2*S1 + S2*S1
C      KK = KK - NT + JC
C      IF (KK.LE. KSPAN) GO TO 420
C      KK = KK - KSPAN + INC
C      IF (KK.LE. JC) GO TO 410
C      IF (KSPAN.EQ. JC) GO TO 800
C      GO TO 100
C      450 AKP = AKM + BJM
C      AKM = AKM - BJM
C      BKP = BKM - AJM
C      BKM = BKM + AJM
C      IF (S1.NE. 0.0) GO TO 430
C      460 A(K1) = AKP
C      B(K1) = BKP
C      A(K2) = AJP
C      B(K2) = BJP
C      A(K3) = AKM
C      B(K3) = BKM
C      KK = K3 + KSPAN
C      IF (KK.LE. NT) GO TO 420
C      440 GO TO 440

```

TRANSFORM FOR A FACTOR OF 5.

```

CFFFT3790
CFFFT3800
CFFFT3810
CFFFT3820
CFFFT3830
CFFFT3840
CFFFT3850
CFFFT3860
CFFFT3870
CFFFT3880
CFFFT3890
CFFFT3900
CFFFT3910
CFFFT3920
CFFFT3930
CFFFT3940
CFFFT3950
CFFFT3960
CFFFT3970
CFFFT3980
CFFFT3990
CFFFT4000
CFFFT4010
CFFFT4020
CFFFT4030
CFFFT4040
CFFFT4050
CFFFT4060
CFFFT4070
CFFFT4080
CFFFT4090
CFFFT4100
CFFFT4110
CFFFT4120
CFFFT4130
CFFFT4140
CFFFT4150
CFFFT4160
CFFFT4170
CFFFT4180
CFFFT4190
CFFFT4200
CFFFT4210
CFFFT4220
CFFFT4230
CFFFT4240
CFFFT4250
CFFFT4260

```



```

510 C2 = C72**2 - S72**2
S2 = 2.0 * C72 * S72
C
520 K1 = KK + KSPAN
K2 = K1 + KSPAN
K3 = K2 + KSPAN
K4 = K3 + KSPAN
C
AKP = A(K1) + A(K4)
AKM = A(K1) - A(K4)
BKM = B(K1) + B(K4)
BKM = B(K1) - B(K4)
C
AJP = A(K2) + A(K3)
AJM = A(K2) - A(K3)
EJM = B(K2) + B(K3)
BJM = B(K2) - B(K3)
C
AA = A(KK)
BE = B(KK)
A(KK) = AA + AKP + AJP
B(KK) = BB + BKP + BJP
C
AK = AKP * C72 + AJP * C2 + AA
BK = BKP * C72 + BJP * C2 + BB
AJ = AKM * S72 + AJM * S2
BJ = BKM * S72 + BJM * S2
C
A(K1) = AK - BJ
A(K4) = AK + BJ
B(K1) = BK + AJ
B(K4) = BK - AJ
C
AK = AKP * C2 + AJP * C72 + AA
BK = BKP * C2 + BJP * C72 + BB
AJ = AKM * S2 - AJM * S72
BJ = BKM * S2 - BJM * S72
C
A(K2) = AK - BJ
A(K3) = AK + BJ
B(K2) = BK + AJ
B(K3) = BK - AJ
KK = K4 + KSPAN
C
IF (KK .LT. NN) GO TO 520
KK = KK - NN
C
IF (KK .LE. KSPAN) GO TO 520

```



```

C
C      GO TO 700
C      TRANSFORM FOR ODD FACTORS.
C
C      600 K = NFAC(I)
C          KSPNN = KSPAN
C          KSPAN = KSPAN/K
C          IF (K .EQ. 3) GO TO 320
C
C          IF (K .EQ. 5) GO TO 510
C
C          IF (K .EQ. JF) GO TO 640
C
C          JF = K
C          S1 = RAD/FLOAT(K)
C          C1 = COS(S1)
C          S1 = SIN(S1)
C          IF (JF .GT. MAXF) GO TO 998
C
C          CK(JF) = 1.0
C          SK(JF) = 0.0
C          J = 1
C
C          630 CK(J) = CK(K) * C1 + SK(K) * S1
C              SK(J) = CK(K) * S1 - SK(K) * C1
C
C              K = K - 1
C              CK(K) = CK(J)
C              SK(K) = -SK(J)
C
C              J = J + 1
C              IF (J .LT. K) GO TO 630
C
C          640 K1 = KK
C              K2 = KK + KSPNN
C
C              AA = A(KK)
C              BB = B(KK)
C              AK = AA
C              BK = BB
C
C              J = 1
C              K1 = K1 + KSPAN
C
C          650 K2 = K2 - KSPAN
C              J = J + 1
C
C              AT(J) = A(K1) + A(K2)

```

```

CFFT4750
CFFT4760
CFFT4770
CFFT4780
CFFT4790
CFFT4800
CFFT4810
CFFT4820
CFFT4830
CFFT4840
CFFT4850
CFFT4860
CFFT4870
CFFT4880
CFFT4890
CFFT4900
CFFT4910
CFFT4920
CFFT4930
CFFT4940
CFFT4950
CFFT4960
CFFT4970
CFFT4980
CFFT4990
CFFT5000
CFFT5010
CFFT5020
CFFT5030
CFFT5040
CFFT5050
CFFT5060
CFFT5070
CFFT5080
CFFT5090
CFFT5100
CFFT5110
CFFT5120
CFFT5130
CFFT5140
CFFT5150
CFFT5160
CFFT5170
CFFT5180
CFFT5190
CFFT5200
CFFT5210
CFFT5220

```



```

CFFT5230
CFFT5240
CFFT5250
CFFT5260
CFFT5270
CFFT5280
CFFT5290
CFFT5300
CFFT5310
CFFT5320
CFFT5330
CFFT5340
CFFT5350
CFFT5360
CFFT5370
CFFT5380
CFFT5390
CFFT5400
CFFT5410
CFFT5420
CFFT5430
CFFT5440
CFFT5450
CFFT5460
CFFT5470
CFFT5480
CFFT5490
CFFT5500
CFFT5510
CFFT5520
CFFT5530
CFFT5540
CFFT5550
CFFT5560
CFFT5570
CFFT5580
CFFT5590
CFFT5600
CFFT5610
CFFT5620
CFFT5630
CFFT5640
CFFT5650
CFFT5660
CFFT5670
CFFT5680
CFFT5690
CFFT5700

```

```

C      AK = AT(J) + AK
      BT(J) = B(K1) + B(K2)
      BK = BT(J) + BK
      J = J+1
C
C      AT(J) = A(K1) - A(K2)
      BT(J) = B(K1) - B(K2)
C
C      K1 = K1 + KSPAN
      IF (K1.LT.K2) GO TO 650
C
C      A(KK) = AK
      B(KK) = BK
C
C      K1 = KK
      K2 = KK + KSPNN
      J = 1
C
C      66C  K1 = K1 + KSPAN
           K2 = K2 - KSPAN
           JJ = J
C
C      AK = AA
      BK = BB
      AJ = 0.0
      BJ = 0.0
      K = 1
C
C      670  K = K + 1
           AK = AT(K) * CK(JJ) + AK
           BK = BT(K) * CK(JJ) + BK
C
C      K = K + 1
      AJ = AT(K) * SK(JJ) + AJ
      BJ = BT(K) * SK(JJ) + BJ
C
C      JJ = JJ + J
      IF (JJ.GT.JF) JJ = JJ - JF
C
C      IF (K.LT.JF) GO TO 670
C
C      K = JF - J
      A(K1) = AK - BJ
      B(K1) = BK + AJ
C
C      A(K2) = AK + BJ
      B(K2) = BK - AJ

```



```

C      J = J + 1
C      IF (J .LT. K) GO TO 660
C      KK = KK + KSPNN
C      IF (KK .LE. NN) GO TO 640
C      KK = KK - NN
C      IF (KK .LE. KSPAN) GO TO 640
C      MULTIPLY BY ROTATION FACTOR (EXCEPT FOR FACTORS OF 2 AND 4).
C      700 IF (I .EQ. M) GO TO 800
C      KK = JC + 1
C      710 C2 = 1.0 - CD
C      S1 = SD
C      720 C1 = C2
C      S2 = S1
C      KK = KK + KSPAN
C      730 AK = A(KK)
C      A(KK) = C2 * AK - S2 * B(KK)
C      B(KK) = S2 * AK + C2 * B(KK)
C      KK = KK + KSPNN
C      IF (KK .LE. NT) GO TO 730
C      AK = S1 * S2 + C1 * S2
C      S2 = S1 * C2 - AK
C      KK = KK - NT + KSPAN
C      IF (KK .LE. KSPNN) GO TO 730
C      C2 = C1 - (CD * C1 + SD * S1)
C      S1 = S1 + (SD * C1 - CD * S1)
C      C1 = 0.5 / (C2**2 + S1**2) + 0.5
C      S1 = C1 * S1
C      C2 = C1 * C2
C      KK = KK - KSPNN + JC
C      IF (KK .LE. KSPAN) GO TO 720
C      KK = KK - KSPAN + JC + INC
C      IF (KK .LE. JC + JC) GO TO 710
C      CC TO 100

```

```

CFFFT5710
CFFFT5720
CFFFT5730
CFFFT5740
CFFFT5750
CFFFT5760
CFFFT5770
CFFFT5780
CFFFT5790
CFFFT5800
CFFFT5810
CFFFT5820
CFFFT5830
CFFFT5840
CFFFT5850
CFFFT5860
CFFFT5870
CFFFT5880
CFFFT5890
CFFFT5900
CFFFT5910
CFFFT5920
CFFFT5930
CFFFT5940
CFFFT5950
CFFFT5960
CFFFT5970
CFFFT5980
CFFFT5990
CFFFT6000
CFFFT6010
CFFFT6020
CFFFT6030
CFFFT6040
CFFFT6050
CFFFT6060
CFFFT6070
CFFFT6080
CFFFT6090
CFFFT6100
CFFFT6110
CFFFT6120
CFFFT6130
CFFFT6140
CFFFT6150
CFFFT6160
CFFFT6170
CFFFT6180

```



```

C      PERMUTE RESULTS TO NORMAL ORDER IN TWO STAGES:
C      PERMUTATION FOR SQUARE FACTORS OF N
C
C      800 NP(1) = KS
C      IF (KT .EQ. 0) GO TO 890
C
C      K = KT + KT + 1
C      IF (M .LT. K) K = K - 1
C
C      J = 1
C      NP(K+1) = JC
C
C      810 NP(J+1) = NP(J)/NFAC(J)
C      NP(K) = NP(K+1) * NFAC(J)
C
C      J = J + 1
C      K = K - 1
C      IF (J .LT. K) GO TO 810
C
C      K3 = NP(K+1)
C      KSPAN = NP(2)
C      KK = JC + 1
C      K2 = KSPAN + 1
C
C      J = 1
C      IF (N .NE. NTOT) GO TO 850
C
C      PERMUTATION FOR SINGE-VARIATE TRANSFORM
C
C      820 AK = A(KK)
C      A(KK) = A(K2)
C      A(K2) = AK
C
C      BK = B(KK)
C      B(KK) = B(K2)
C      B(K2) = BK
C
C      KK = KK + INC
C      K2 = KSPAN + K2
C      IF (K2 .LT. KS) GO TO 820
C
C      830 K2 = K2 - NP(J)
C      J = J + 1
C      K2 = NP(J+1) + K2
C      IF (K2 .GT. NP(J)) GO TO 830
C      J = 1

```

CFFT6190
 CFFT6200
 CFFT6210
 CFFT6220
 CFFT6230
 CFFT6240
 CFFT6250
 CFFT6260
 CFFT6270
 CFFT6280
 CFFT6290
 CFFT6300
 CFFT6310
 CFFT6320
 CFFT6330
 CFFT6340
 CFFT6350
 CFFT6360
 CFFT6370
 CFFT6380
 CFFT6390
 CFFT6400
 CFFT6410
 CFFT6420
 CFFT6430
 CFFT6440
 CFFT6450
 CFFT6460
 CFFT6470
 CFFT6480
 CFFT6490
 CFFT6500
 CFFT6510
 CFFT6520
 CFFT6530
 CFFT6540
 CFFT6550
 CFFT6560
 CFFT6570
 CFFT6580
 CFFT6590
 CFFT6600
 CFFT6610
 CFFT6620
 CFFT6630
 CFFT6640
 CFFT6650
 CFFT6660


```

      840 IF (KK .LT. K2) GO TO 820
      C
      KK = KK + INC
      K2 = KSPAN + K2
      IF (K2 .LT. KS) GO TO 840
      C
      IF (KK .LT. KS) GO TO 830
      C
      JC = K3
      GC TO 850
      C
      PERMUTATION FOR MULTIVARIATE TRANSFORM
      C
      850 K = KK + JC
      C
      860 AK = A(KK)
      A(KK) = A(K2)
      A(K2) = AK
      C
      BK = B(KK)
      B(KK) = B(K2)
      B(K2) = BK
      C
      KK = KK + INC
      K2 = K2 + INC
      IF (KK .LT. K) GO TO 860
      C
      KK = KK + KS - JC
      K2 = K2 + KS - JC
      IF (KK .LT. NT) GO TO 850
      C
      K2 = K2 - NT + KSPAN
      KK = KK - NT + JC
      IF (K2 .LT. KS) GO TO 850
      C
      870 K2 = K2 - NP(J)
      J = J + 1
      C
      K2 = NP(J+1) + K2
      IF (K2 .GT. NP(J)) GO TO 870
      J = 1
      C
      880 IF (KK .LT. K2) GO TO 850
      KK = KK + JC
      K2 = KSPAN + K2
      C
      IF (K2 .LT. KS) GO TO 880
      C

```

```

CFFT6670
CFFT6680
CFFT6690
CFFT6700
CFFT6710
CFFT6720
CFFT6730
CFFT6740
CFFT6750
CFFT6760
CFFT6770
CFFT6780
CFFT6790
CFFT6800
CFFT6810
CFFT6820
CFFT6830
CFFT6840
CFFT6850
CFFT6860
CFFT6870
CFFT6880
CFFT6890
CFFT6900
CFFT6910
CFFT6920
CFFT6930
CFFT6940
CFFT6950
CFFT6960
CFFT6970
CFFT6980
CFFT6990
CFFT7000
CFFT7010
CFFT7020
CFFT7030
CFFT7040
CFFT7050
CFFT7060
CFFT7070
CFFT7080
CFFT7090
CFFT7100
CFFT7110
CFFT7120
CFFT7130
CFFT7140

```



CFFT7150
 CFFT7160
 CFFT7170
 CFFT7180
 CFFT7190
 CFFT7200
 CFFT7210
 CFFT7220
 CFFT7230
 CFFT7240
 CFFT7250
 CFFT7260
 CFFT7270
 CFFT7280
 CFFT7290
 CFFT7300
 CFFT7310
 CFFT7320
 CFFT7330
 CFFT7340
 CFFT7350
 CFFT7360
 CFFT7370
 CFFT7380
 CFFT7390
 CFFT7400
 CFFT7410
 CFFT7420
 CFFT7430
 CFFT7440
 CFFT7450
 CFFT7460
 CFFT7470
 CFFT7480
 CFFT7490
 CFFT7500
 CFFT7510
 CFFT7520
 CFFT7530
 CFFT7540
 CFFT7550
 CFFT7560
 CFFT7570
 CFFT7580
 CFFT7590
 CFFT7600
 CFFT7610
 CFFT7620

```

      IF (KK .LT. KS) GO TO 870
      JC = K3
      C 850 IF (2 * KT + 1 .GE. M) RETURN
      C      KSPNN = NP(KT+1)
      C      PERMUTATION FOR SQUARE-FREE FACTORS CF N.
      C      J = M - KT
      C      NFAC(J+1) = 1
      C 900 NFAC(J) = NFAC(J) * NFAC(J+1)
      C      J = J - 1
      C      IF (J .NE. KT) GO TO 900
      C      KT = KT + 1
      C      NN = NFAC(KT) - 1
      C      IF (NN .GT. MAXP) GO TO 998
      C      JJ = 0
      C      J = 0
      C      GC TO 906
      C 902 JJ = JJ - K2
      C      K2 = KK
      C      K = K + 1
      C      KK = NFAC(K)
      C 904 JJ = KK + JJ
      C      IF (JJ .GE. K2) GO TO 902
      C      NP(J) = JJ
      C 906 K2 = NFAC(KT)
      C      K = KT + 1
      C      KK = NFAC(K)
      C      J = J + 1
      C      IF (J .LE. NN) GO TO 904
      C      DETERMINE PERMUTATION CYCLES CF LENGTH .GT. 1
      C      J = 0
      C      GO TO 914
      C 910 K = KK
      C      KK = NP(K)
  
```



```

      NP(K) = -KK
      IF (KK.NE. J) GO TO 910
      K 3 = KK
C 914 J = J + 1
      KK = NP(J)
      IF (KK.LT. 0) GO TO 914
C      IF (KK.NE. J) GO TO 910
C
      NP(J) = -J
      IF (J.NE. NN) GO TO 914
      MAXF = INC * MAXF
C      REORDER A AND B, FOLLOWING PERMUTATION CYCLES.
C      GO TO 950
C
C 924 J = J - 1
      IF (NP(J).LT. 0) GO TO 924
      JJ = JC
C
C 926 KSPAN = JJ
      IF (JJ.GT. MAXF) KSPAN = MAXF
C
      JJ = JJ - KSPAN
      K = NP(J)
      KK = JC * K + II + JJ
      K1 = KK + KSPAN
      K2 = 0
C
C 928 K2 = K2 + 1
      AT(K2) = A(K1)
      BT(K2) = B(K1)
C
      K1 = K1 - INC
      IF (K1.NE. KK) GO TO 928
C
C 932 K1 = KK + KSPAN
      K2 = K1 - JC * (K+NP(K))
      K = -NP(K)
C
C 936 A(K1) = A(K2)
      B(K1) = B(K2)
C
      K1 = K1 - INC
      K2 = K2 - INC
      IF (K1.NE. KK) GO TO 936

```

```

CFFT7630
CFFT7640
CFFT7650
CFFT7660
CFFT7670
CFFT7680
CFFT7690
CFFT7700
CFFT7710
CFFT7720
CFFT7730
CFFT7740
CFFT7750
CFFT7760
CFFT7770
CFFT7780
CFFT7790
CFFT7800
CFFT7810
CFFT7820
CFFT7830
CFFT7840
CFFT7850
CFFT7860
CFFT7870
CFFT7880
CFFT7890
CFFT7900
CFFT7910
CFFT7920
CFFT7930
CFFT7940
CFFT7950
CFFT7960
CFFT7970
CFFT7980
CFFT7990
CFFT8000
CFFT8010
CFFT8020
CFFT8030
CFFT8040
CFFT8050
CFFT8060
CFFT8070
CFFT8080
CFFT8090
CFFT8100

```



```

C      KK = K2
C      IF (K .NE. J) GO TO 932
C
C      K1 = KK + KSPAN
C      K2 = 0
C
C      940 K2 = K2 + 1
C      A(K1) = AT(K2)
C      B(K1) = BT(K2)
C
C      K1 = K1 + INC
C      IF (K1 .NE. KK) GO TO 940
C
C      IF (JJ .NE. 0) GO TO 926
C
C      IF (J .NE. 1) GO TO 924
C
C      950 J = K3 + 1
C      NT = NT - KSPNN
C      II = NT - INC + 1
C      IF (NT .GE. 0) GO TO 924
C
C      RETURN
C
C      ERROR TERMINATION: INS
C
C      998 ISN = 0
C      STOP 999
C      END

```



```

** ** ** ** ** ** ** ** ** ** **  1) FT02F001 - OUTPUT IN FORM TO BE READ BACK INTO
** ** ** **  PROGRAM UNDER MODE 3 OPERATION (CHANGE MODE=1
** ** ** **  TO MODE=3 ON THE 4TH DATA CARD
** ** ** **  2) FT03F001 - OUTPUT AS PRINTED UNDER CS
** ** ** **  *****
** ** ** **  MAIN COMPUTER PROGRAM
** ** ** **  *****
** ** ** **  INTEGRAL INVERSION
** ** ** **  *****
** ** **  REFERENCE, THESIS BY P. E. VAN HOUTEN, THE APPLICATION OF
** ** **  HOLOGRAPHIC INTERFEROMETRY DENSITY FIELD, 14 DEC 72, DISCUSS-
** ** **  TINUCUS THREE-DIMENSIONAL A CIRCULAR REGION OF UNKNOWN LENGTH
** ** **  THE PROGRAM CONSIDERS WHICH THE TOTALY PLASE SHIFT (PATH LENGTH
** ** **  REFRACTIVE) INDEX FOR NUMERICAL SPACES AT REGULAR INTERVALS
** ** **  DIFFERENCE) IS KNOWN ANGLE. THE PROGRAM REQUIRES ANGLE
** ** **  FOR A GIVEN REGULAR SPACED INTERVALS AND A TOTAL ANGLE
** ** **  VIEWS AT REGULAR SPACED INTERVALS. THE NECESSARY ANGULAR
** ** **  COVERAGE OF 180 DEGREES (ASYMMETRIC). THE NECESSARY ANGULAR
** ** **  COVERAGE IS REDUCED BY THE NUMBER OF DEGREES OF SYMMETRY.
** ** **  BY THE USE OF TWO DIMENSIONAL FOURIER TRANSFORM TECHNIQUES
** ** **  IT CAN BE SHOWN THAT FOR A GIVEN POINT (X0,Y0) WITHIN THE
** ** **  CIRCULAR REGION, THE DENSITY INFORMATION CAN BE EXPRESSED IN
** ** **  TERMS OF THE PHASE SHIFT INFORMATION G(RC, THETA).
** ** **  INSIDE IN ORDER TO SAVE COMPUTATION TIME, THE VALUE OF THE EACH
** ** **  VIEWING INTEGRATION IS COMPUTED AT EACH, RAY POSITION FOR THE
** ** **  VIEWING ANGLE. FOR A GIVEN POINT (X0,Y0), THE VALUE OF THE
** ** **  INSIDE INTEGRAL IS DETERMINED BY AVERAGING OVER A FINITE
** ** **  PARTITION OF A CUBIC POLYNOMIAL. FITTED TO THE FOUR CLOSEST
** ** **  VALUES OF THE INSIDE INTEGRAL. THE INTEGRATION OVER THETA
** ** **  USES THE TRAPEZOIDAL RULE. THE INTEGRATION OVER RHO USES
** ** **  COTES SIXTH ORDER QUADRATURE FORMULA
** ** **  *****
** ** **  MEANING OF SYMBOLS USED IN THE PROGRAM
** ** **  *****
** ** **  IT(12) TITLE USED FOR OUTPUT. FIRST 48 CHARACTERS CN FIRST
** ** **  DATA CARD, FIRST 16 CHARACTERS CN NEXT DATA CARD
** ** **  RHOINF-DENSITY CUT SIDE REGION CF INTEREST IN MG/CC.
** ** **  XLAMDA-WAVELENGTH OF MONOCHROMATIC, COHERENT LIGHT SOURCE IN

```



```

*EVE000430
*EVE000440
*EVE000450
*EVE000460
*EVE000470
*EVE000480
*EVE000490
*EVE000500
*EVE000510
*EVE000520
*EVE000530
*EVE000540
*EVE000550
*EVE000560
*EVE000570
*EVE000580
*EVE000590
*EVE000600
*EVE000610
*EVE000620
*EVE000630
*EVE000640
*EVE000650
*EVE000660
*EVE000670
*EVE000680
*EVE000690
*EVE000700
*EVE000710
*EVE000720
*EVE000730
*EVE000740
*EVE000750
*EVE000760
*EVE000770
*EVE000780
*EVE000790
*EVE000800
*EVE000810
*EVE000820
*EVE000830
*EVE000840
*EVE000850
*EVE000860
*EVE000870
*EVE000880
*EVE000890
*EVE000900

```

```

MICRCNS. AND XLAMDA CN THIRD DATA CARD IN (2F10.5) FORMAT
RHOINF AND XMODE=1 REFRACTIVE INDEX SUPPLIED THROUGH SUBROUTINE
MODE INPUT. THE PROGRAM GENERATES FRINGE DATA
AND RECOMPUTES THE REFRACTIVE INDEX FROM
THE GENERATE FRINGE DATA. AT GRID POINTS
MODE=2 REFRACTIVE INDEX SUPPLIES AS IN MODE 1
BY INPUT DATA. PROGRAM PROCEEDS AS IN MODE 1
MODE=3 FRINGE DATA SUPPLIED, PROGRAM GENERATES
DENSITY FIELD.
MODE=4 SAME AS MODE=3 EXCEPT FRINGE DATA IS RECOM-
PUTED AS PER DATA POINTS
NP NUMBER OF EQUALLY SPACED
NT NUMBER OF VIEWS SUPPLIED
KSYM SYMMETRY OF FIELD 0-4 AXIS OF SYMMETRY
4 -98 DATA REPEATS EVERY KSYM
CEGREES. FIELD
99 AXIS SYMMETRIC FIELD
RMAX RADIUS OF CIRCULAR REGION IN CENTIMETERS
FILTER=(0.-1.) DETERMINES SPAN OVER WHICH AVERAGING OCCURS
THE INFORMATION ON THE FOURTH DATA CARD(411C,2F10.5).
X(I) VECTOR OF GRID POINTS ALONG THETA = 0 DEGREES
X(1)=-RMAX X(NP)=+RMAX
Y(J) VECTOR OF GRID POINTS ALONG THETA=90 DEGREES
Y(1)=-RMAX Y(NP)=+RMAX
A(I,J) DENSITY OR REFRACTIVE INDEX AT THE POINT X(I),Y(J).
RB(I) VECTOR OF POINTS ON THE PHOTOGRAPHIC PLATE RB(1)=-2 RMAX
RB(2 NP)=2 RMAX. GRID SPACING OF RAYS. DR=2*RMAX/(NP-1)
DR SPACING OF VIEWING ANGLES IN DEGREES
TH(K) VECTOR OF SHIFT INFORMATION AT THE POINT(RB(I),TH(K)).
B(I,K) FRINGED INTENSITY BB(I,K). THE VALUE OF THE INSIDE
B(I,K) IS COPIED INTO BB(I,K). IN B(I,K).
INTEGRATION IS THEN STORED IN B(I,K). 0 NC SYMMETRY
DASYM(K) SYMMETRY OF DATA(B(I,K). 1 DATA SYMMETRIC ABOUT RB=0.
IF DASYM = 1.0 ONLY (NP+1)/2 DATA POINTS SHOULD BE FURNISHED.
BD(L) IS A VECTOR USED BY THE PROGRAM.
FOR MODE=1 OR MODE=2 THE FIFTH DATA CARD IS THE VECTOR
TH(K) IN (8F10.5) FORMAT
FOR MODE 2 OPERATION THE REFRACTIVE INDEX FOLLOWS IN 8F10.5
FOR MODE=3 AND MODE=4 OPERATION, THE FIFTH DATA CARD IS
TH(1) AND DASYM(1) IN (2F10.5) FORMAT. THIS IS FOLLOWED
BY THE FRINGE INFORMATION FOR THAT VIEW. (B(1,1) ETC UNTIL
ALL VIEWS AND FRINGE SHIFT HAS BEEN SUPPLIED
IF AXIS OF SYMMETRY EXISTS, THETA=0. MUST CORRESPOND TO ONE OF
THE AXIS OF SYMMETRY.

```

CC


```

C*****ZERO MATRICES AND SET GRID *****
C
DO 2 I=1,NP
DO 1 J=1,NP
1 A(I,J)=0.0
2 B(I,K)=0.0
2 B(I,K)=0.0
2 X(I)=RMAX
Y(I)=X(I)
DO 3 I=2,NP
X(I)=X(I-1)+DR
3 Y(I)=X(I)
C*****READ VIEWING ANGLES AND SET SIN AND COSINE FOR MODE=1,2*****
C
4 READ(1,103) (TH(K),K=1,NT)
DO 5 K=1,NT
THETA=TH(K)/57.296
CC(K)=CCS(THETA)
SS(K)=SIN(THETA)
5 IF(KSYM.EQ.99) GO TO 13
C*****SET REFRACTIVE INDEX AND WRITE SAME FOR NCCE CNE OPERATION*****
C
DO 8 I=1,NP
DO 8 J=1,NP
XI=X(I)
YJ=Y(J)
CALL INPUT(XI,YJ,VAL)
8 5 A(I,J)=VAL
5 WRITE(8,115)
WRITE(8,113)
K=1
K21=21
11 WRITE(8,106) (X(I),I=K,K21)
WRITE(8,110)
DO 12 I=1,NP
NN=NP-I+1
12 WRITE(8,111) Y(NN),A(J,NN),J=K,K21)
IF(K21.EQ.NP) GO TO 15
K=K21+1
K21=K21+21
IF(K21.GT.NP) K21=NP
GO TO 11
C*****
C*****SET REFRACTIVE INDEX FOR AXISYMETRIC CASE*****
C
C*****
C*****

```

```

VE01390
VE01400
VE01410
VE01420
VE01430
VE01440
VE01450
VE01460
VE01470
VE01480
VE01490
VE01500
VE01510
VE01520
VE01530
VE01540
VE01550
VE01560
VE01570
VE01580
VE01590
VE01600
VE01610
VE01620
VE01630
VE01640
VE01650
VE01660
VE01670
VE01680
VE01690
VE01700
VE01710
VE01720
VE01730
VE01740
VE01750
VE01760
VE01770
VE01780
VE01790
VE01800
VE01810
VE01820
VE01830
VE01840
VE01850
VE01860

```



```

38 BB(K,I)=-3.*Q2+RB(K)*(3.*Q2+4.*C1/3.+RB(K)*(-Q2/1.5-C1/2.25))
DC 381 I=1,NT
DC 382 J=1,NPP
WRITE(3,1001) BB(J,I),J,I
1001 FCRMAT(F10.5,2I10)
382 CCNTINUE
381 CCNTINUE
C *****
C *****
C *****
C *****CALCULATE VALUE OF INSIDE INTEGRAL *****
C *****
DC 43 I=1,NT
DC 43 J=1,NP
M=NPL+J
BD(1)=0.
CC 39 K=1,MAX
MKP=M+K
MKM=M-K
IF(MKP.GT.NPP) MKP=NPP
IF(MKM.LT.1) MKM=1
K1=K**2
39 BC(K+1)=(BB(MKP,I)+BB(MKM,I)-2.*BB(M,I))/(FLCAT(K1)*CR)
IF(J.GT.20) GO TO 391
WRITE(3,1002) (BD(L),L=1,98)
1002 FCRMAT(10F8.3)
391 CCNTINUE
VAL=0.
K1=1
40 K2=K1+6
IF(K2.GT.MAX) GO TO 41
CCIES SIXTH ORDER QUADATURE FORMULA*****
VAL=VAL+C1*(BD(K1)+BD(K2))+C2*(BD(K1+1)+BD(K2-1))+C3*(BD(K1+2)+BD(K2-2))+C4*BD(K1+3)
K1=K2
GO TO 40
41 SUM=0.
CCNTIRIBUTION OF LAST TERMS
DO 42 K=K1,MAX
SUM=SUM+BD(K)+BD(K+1)
42 SUM=COTES PLUS LAST TERMS PLUS INTEGRATION FROM 2 RMAX TO INFINITY
B(J,I)= VAL+SUM/2.-.666667*BB(M,I)/RMAX
WRITE(3,1001) B(J,I),J,I
43 CCNTINUE
IF(KSYM.LT.99) GO TO 48
C *****

```

```

EVE02350
EVE02360
EVE02370
EVE02380
EVE02390
EVE02400
EVE02410
EVE02420
EVE02430
EVE02440
EVE02450
EVE02460
EVE02470
EVE02500
EVE02510
EVE02520
EVE02530
EVE02540
EVE02550
EVE02560
EVE02570
EVE02580
EVE02590
EVE02600
EVE02610
EVE02620
EVE02630
EVE02640
EVE02650
EVE02660
EVE02670
EVE02680
EVE02690
EVE02700
EVE02710
EVE02720
EVE02730
EVE02740
EVE02750
EVE02760
EVE02770
EVE02780
EVE02790
EVE02800
EVE02810
EVE02820
EVE02830
EVE02840

```



```

C REFRACTIVE INDEX SUPPLIED*****
GC TO 75
CCCONTINUE
48 M=NT+1
IF(KSYM.EQ.0) GO TO 51
IF(KSYM.GT.4) GO TO 53
C*****GENERATE ADDITIONAL DATA DEPENDING ON SYMETRY OF FIELD*****
C
C DT=TH(2)-TH(1)
NTP=NT
DO 50 J=1,KSYM
K=J*NT
DO 49 I=1,NTP
KK=K+I
TH(KK)=TH(KK-1)+DT
KM=K-I+1
DC 49 L=1,NP
45 B(L,KK)=B(L,KM)
50 NTP=2*NTP
M=KK+1
C*****GENERATE DATA FOR 180 DEGREE VIEW*****
C
C 51 TH(M)=TH(1)+180.
DC 52 I=1,NP
K=(NP-I+1)
52 B(K,M)=B(I,1)
C*****
C
C GC TO 55
C*****GENERATE ADDITIONAL DATA FOR REPEATING DATA*****
C
C 53 M=180/KSYM+1
DC 54 I=2,M
TH(I)=TH(I-1)+FLOAT(KSYM)
DC 54 J=1,NP
54 B(J,I)=B(J,I-1)
55 CCCONTINUE
C*****
C
C*****INTEGRATE ON THETA FOR ASYMETRIC FIELD*****
C
C
C
C

```

```

EVE03330
EVE03340
EVE03350
EVE03380
EVE03390
EVE03400
EVE03410
EVE03420
EVE03430
EVE03440
EVE03450
EVE03460
EVE03470
EVE03480
EVE03490
EVE03500
EVE03510
EVE03520
EVE03530
EVE03540
EVE03550
EVE03560
EVE03570
EVE03580
EVE03590
EVE03600
EVE03610
EVE03620
EVE03630
EVE03640
EVE03650
EVE03660
EVE03670
EVE03680
EVE03690
EVE03700
EVE03710
EVE03720
EVE03730
EVE03740
EVE03750
EVE03760
EVE03770
EVE03780
EVE03790
EVE03800
EVE03810
EVE03820

```



```

MD=M-1/(2.*3.1416*FLOAT(MD))
DEL=-1.
DO 56 I=1,M
  CC(I)=COS(TH(I)/57.296)
  SS(I)=SIN(TH(I)/57.296)
56 DO 61 LL=1,NP
  J=NP+1-LL
  DC 60 I=1,NP
  A(I,J)=0.
  DC 58 K=1,M
  R=Y(J)*CC(K)-X(I)*SS(K)
  NN=(R+RMAX+DR)/DR
  IF(NN*GE.NP) GO TO 60
  IF(NN*LT.1) GO TO 60
  LP1=NN+1
  LM1=NN-1
  IF(LP2*GT.NP) LP2=NP
  IF(LM1*LT.1) LM1=1
  P=(R-X(NN))/DR
  COF3=.1666666*(B(LP2,K)-B(LP1,K))-5*(B(LP1,K)-B(NN,K))
  COF2=-.5*(B(LP1,K)+B(LP2,K))-3333333*B(LP1,K)-.5*B(NN,K)
  CCFL=-.1666666*B(LP2,K)-.3333333*B(LP1,K)-.5*B(NN,K)
  P2=P*P
C*****AMOUNT OF FILTERING DEPENDS ON FT2=FILTER*FILTER*****
58 BD(K)=P*(P2+FT2)*COF3+(P2+.666666*FT2)*COF2+P*COF1+B(NN,K)
C INTEGRATE OVER THETA USING TRAPEZOIDAL INTEGRATION*****
  VAL=0.0
  DO 59 L=2,M
    VAL=VAL+BD(L)+BD(L-1)
59 A(I,J)=VAL*DEL/2.
C*****
60 CCNTINUE
61 CCNTINUE
C*****
C*****
NPN=NP+NPL
IF(MODE*LT.4) GO TO 63
63 IF(MODE*LT.3) GO TO 65
C*****CHANGE REFRACTIVE INDEX FIELD TO DENSITY FIELD*****
DC 64 I=1,NP
DC 64 J=1,NP
64 A(I,J)=RHOINF+.4443*XLAMD*A(I,J)
C*****
C*****

```



```

WRITE(8,114)
GO TO 66
65 WRITE(8,115)
66 WRITE(8,113)
C
C*****WRITE REFRACTIVE INDEX OR DENSITY FIELD*****
C
K=1
K21=21
WRITE(8,106) (X(I),I=K,K21)
67 WRITE(8,110) (X(I),I=1,NP)
DC 68 I=1,NP
NN=NP-I+1
68 WRITE(8,111) Y(NN), (A(J,NN),J=K,K21)
IF(K21.EQ.NP) GO TO 69
K=K21+1
K21=K21+21
IF(K21.GT.NP) K21=NP
69 WRITE(8,116)
C
C*****WRITE FRINGE SHIFT INFORMATION*****
C
WRITE(8,104) (TH(K),K=1,NT)
CC 70 I=N,NPN
70 WRITE(8,105) RB(I), (BB(I,J),J=1,NT)
C
WRITE(8,115)
WRITE(8,104) (TH(K),K=1,NT)
DO 700 J=1,NT
WRITE(8,103) TH(J)
WRITE(8,103) (BB(I,J),I=N,NPN)
700 CCNTINUE
C
WRITE(2,112) (IT(I),I=1,12)
WRITE(2,103) RHOINF,XLAM0
WRITE(2,100) MODE,NP,NT,KSYP,RMAX,FILTER
DO 710 J=1,NT
WRITE(2,103) TH(J)
WRITE(2,103) (BB(I,J),I=N,NPN)
710 CCNTINUE
C
WRITE(8,117)
WRITE(8,104) (TH(K),K=1,M)
DC 71 I=1,NP

```


APPENDIX F. ALTERNATE PROGRAMS DESIGNED TO CALCULATE THE INSIDE INTEGRAL

APPENDIX F.1 JONES1--USING CONVOLUTION VALUES OBTAINED NUMERICALLY

See Appendix F.2 for expanded fringe shift information used as input fringe data for $-1.5 \leq R \leq 1.5$

```

DIMENSION X(513),Y(513),Z(513) ,XD(513),YD(513),B(513)
N=512
PY=3.141593
R=12.0
FA=N
DR=2.*R/FN
C*****LIMITS FOR READING DATA AND PRINTING OUTPUTS*****
INTE=1
INTE=65
INTPRB=256
INTPRE=322
NPL=N+1
DO 21 I=1,NPL
  Y(I)=0.0
  21 CCNTINUE
  301 READ (1,301) (Y(M),M=INTB,INTE)
  301 FORMAT(F10.5)
  DO 22 I=1,NPL
    B(I)=0.0
    IF (I.LE. INTPRB) GO TO 22
    IF (I.GE. INTPRE) GO TO 22
    C*****PRINT CHECK FOR PROPER INPUT OF FRINGE DATA*****
    WRITE (4,101) Y(I),B(I),I
    22 CCNTINUE
  DO 5 K=1,NPL
    C=-R+DR*(K-1)
    IF (C.EQ.0.0) GO TO 6
    X(K)=1./C
    GO TO 7
  6 X(K)=0.
  7 CCNTINUE
  IF (K.LE. INTPRB) GO TO 5
  IF (K.GE. INTPRE) GO TO 5
  C*****PRINT CHECK FOR PROPER INPUT OF 1/R VECTOR*****
  WRITE (4,201) X(K),Y(K),K,C
  201 FORMAT(2F10.5,I10,F10.5)
  5 CCNTINUE
  DO 10 I=1,N
    Z(I)=0.0
    DO 9 J=1,I
      Z(I)=Z(I)+X(J)*Y(I+1-J)
    
```

HAL00010
 HAL00020
 HAL00030
 HAL00040
 HAL00050
 HAL00060
 HAL00070
 HAL00080
 HAL00090
 HAL00100
 HAL00110
 HAL00120
 HAL00130
 HAL00140
 HAL00150
 HAL00160
 HAL00170
 HAL00180
 HAL00190
 HAL00200
 HAL00210
 HAL00220
 HAL00230
 HAL00240
 HAL00250
 HAL00260
 HAL00270
 HAL00280
 HAL00290
 HAL00300
 HAL00310
 HAL00320
 HAL00330
 HAL00340
 HAL00350
 HAL00360
 HAL00370
 HAL00380
 HAL00390
 HAL00400
 HAL00410
 HAL00420


```

9 CONTINUE
  Z(I)=Z(I)*DR
  IF (I.LE.INTPRB) GO TO 10
  IF (I.LE.INTPRE) GO TO 10
  PRINT (I, 'CHECK OF VALUE OF NUMERICAL CONVOLUTION*****')
  C****
  101 WRITE(4,101) Y(I), Z(I), I
  1C FORMAT(2F10.5, I10)
  CONTINUE
  CALL CFFT2(Z,B,N,N,N,-1)
  DO 15 I=1,N
    Z(I)=Z(I)/FN
    P(I)=B(I)/FN
    T=2.*PY*(I-1.)/FN
    XD(I)=-SIN(T)*B(I)/DR
    YD(I)=SIN(T)*Z(I)/DR
    IF (I.LE.INTPRB) GO TO 15
    IF (I.LE.INTPRE) GO TO 15
    PRINT (I, 'CHECK OF FOURIER COEFFICIENTS OF CONVOLUTION AND THEIR
    C****
    C****
    501 WRITE(4,501) Z(I), B(I), I, XD(I), YD(I)
    15 FORMAT(2F10.5, I10, 2F10.5)
    CONTINUE
    CALL CFFT2(XD,YD,N,N,N,1)
    DO 30 J=1,N
      WRITE(4,101) XD(J), YD(J), J
      REAL AND IMAGINARY COEFFICIENTS OF THE INSIDE
      C****
      C****
      30 CONTINUE
      DO 35 I=257,321
        C****
        C****
        601 WRITE(3,601) XD(I)
        35 FORMAT (F10.5)
        CONTINUE
        STOP
        END

```

```

HAL000430
HAL000440
HAL000450
HAL000460
HAL000470
HAL000480
HAL000490
HAL000500
HAL000510
HAL000520
HAL000530
HAL000540
HAL000550
HAL000560
HAL000570
HAL000580
HAL000590
HAL000600
HAL000610
HAL000620
HAL000630
HAL000640
HAL000650
HAL000660
HAL000670
HAL000680
HAL000690
HAL000700
HAL000710
HAL000720
HAL000730
HAL000740
HAL000750
HAL000760
HAL000770

```


APPENDIX F.2. JONES2--USING CONVOLUTION VALUES OBTAINED WITH FFT METHODS

See Appendix F.3 for expanded fringe shift information used as input fringe data for

$1.5 \leq R \leq 1.5$

```
DIMENSION A(513), B(513), D(513), FA(513), FB(513), FX(513)
DIMENSION FY(513), XC(513), YC(513), X(513), Y(513), XD(513), YD(513)
PY=3.141592653
```

R=12.0

N=512

FN=N

DR=2.*R/FN

INTB=1

INTE=65

INTPRB=256

INTPRE=322

NPI=N+1

C INITIALIZE VECTORS TO ZERO

```
DO 110 I=1,NPI
```

A(I)=0.0

B(I)=0.0

X(I)=0.0

Y(I)=0.0

110 CONTINUE

C FRINGE DATA STORED IN A(I) FOR I FROM INTB-INTE.

```
DO 120 I=INTB,INTE
```

READ (1,1001) A(I)

1001 FORMAT (F10.5)

120 CONTINUE

C 1/2 STORED IN X(I) FOR I FROM 1,N.

```
DO 130 I=1,N
```

C=-R+DR*(I-1)

IF(C.EQ.0.00) GO TO 9

X(I)=1./C

GO TO 11

9 X(I)=0.0

11 CONTINUE

IF (I.LE. INTPRB) GO TO 130

IF (I.GE. INTPRE) GO TO 130

PRINTOUT CHECK TO ENSURE DATA INPUTTED CORRECTLY.

WRITE (4,101) X(I),Y(I),I,A(I),B(I),C

101 FORMAT (2F10.5,110,3F10.5)

130 CONTINUE

TAKING FFT OF INPUT DATA

C REAL COEFFICIENTS RETURNED AND PLACED IN FA AND FX.

C IMAGINARY COEFFICIENTS RETURNED AND STORED IN FB AND FY.

CALL CFFT2(X,Y,N,N,-1)

HAC000010
HAC000020
HAC000030
HAC000040
HAC000050
HAC000060
HAC000070
HAC000080
HAC000090
HAC000100
HAC000110
HAC000120
HAC000130
HAC000140
HAC000150
HAC000160
HAC000170
HAC000180
HAC000190
HAC000200
HAC000210
HAC000220
HAC000230
HAC000240
HAC000250
HAC000260
HAC000270
HAC000280
HAC000290
HAC000300
HAC000310
HAC000320
HAC000330
HAC000340
HAC000350
HAC000360
HAC000370
HAC000380
HAC000390
HAC000400
HAC000410
HAC000420


```

CALL CFFT2(A,B,N,N,N,-1)
DC 20 J=1,N
FX(J)=X(J)/FN
FY(J)=Y(J)/FN
FA(J)=A(J)/FN
FB(J)=B(J)/FN
IF (J.LE.INTPRB) GO TO 20
IF (J.GE.INTPRE) GO TO 20
C PRINT CHECK OF FOURIER COEFFICIENTS CF FRINGE DATA AND 1/C.
201 WRITE (4,201) FX(J),FY(J),J,FA(J),FB(J)
20 FCRMAT (2F10.5,I10,2F10.5)
20 CCNTINUE=1,N
DC 21 J=1,N
XC(J)=FX(J)*FA(J)-FY(J)*FB(J)
YC(J)=FX(J)*FB(J)+FY(J)*FA(J)
XC(J)=XC(J)*2.*R
YC(J)=YC(J)*2.*R
IF (J.LE.INTPRB) GO TO 21
IF (J.GE.INTPRE) GO TO 21
C PRINT CHECK OF FOURIER COEFFICIENTS OF CONVOLUTION.
301 WRITE (4,301) XC(J),YC(J),J
301 FCRMAT (2F10.5,I10)
301 CCNTINUE=1,N
DC 22 J=1,N
T=2.*PY*(J-1)/FN
XC(J)=-SIN(T)*YC(J)/DR
YC(J)=SIN(T)*XC(J)/DR
IF (J.LE.INTPRB) GO TO 22
IF (J.GE.INTPRE) GO TO 22
C PRINT CHECK OF DIFFERENTIATION OF FOURIER COEFFICIENTS OF CONVOLUTION
401 WRITE (4,401) XD(J),YD(J),J
401 FCRMAT (2F10.5,I10)
401 CCNTINUE=1,N
DC 30 K=1,N
CALL CFFT2 (XD,YD,N,N,N,1)
WRITE (4,301) XD(K),YD(K),K
C PRINT OUT CF VALUES OF INSIDE INTEGRAL.
C FIRST, Q. POINTS ARE INVALID.
30 CCNTINUE=257,321
DC 35 I=257,321
WRITE (3,601) XD(I)
601 FCRMAT (F10.5)
601 CCNTINUE
35 CALL CFFT2 (XC,YC,N,N,N,1)
C CBTAINING THE INVERSE DFT OF FOUR. COEFF. OF CONVOLUTION.
DC 40 L=1,N
IF (L.LE.INTPRB) GO TO 40
IF (L.GE.INTPRE) GO TO 40

```

HAC00430
HAC00440
HAC00450
HAC00460
HAC00470
HAC00480
HAC00490
HAC00500
HAC00510
HAC00520
HAC00530
HAC00540
HAC00550
HAC00560
HAC00570
HAC00580
HAC00590
HAC00600
HAC00610
HAC00620
HAC00630
HAC00640
HAC00650
HAC00660
HAC00670
HAC00680
HAC00690
HAC00700
HAC00710
HAC00720
HAC00730
HAC00740
HAC00750
HAC00760
HAC00770
HAC00780
HAC00790
HAC00800
HAC00810
HAC00820
HAC00830
HAC00840
HAC00850
HAC00860
HAC00870
HAC00880
HAC00890
HAC00900

HAC00910
HAC00920
HAC00930
HAC00940
HAC00950

C WRITE (4,401) XC(L),YC(L),L
 REAL COEFF: ARE IN FIRST COLUMN, IMAG. COEF. IN SECOND COL.
4C CONTINUE
 STOP
 END

APPENDIX F.3. EXPANDED FRINGE SHIFT INFORMATION USED IN JONES1 AND JONES2

This data was obtained from Van Houten's computer program for MODE ONE operation using control cards as explained in Van Houten's thesis [17] for the asymmetric Gaussian case with $N = 65$ and $R = 1.5$.

0.0
0.0
0.0
0.0
0.0
0.0
-0.11330
-0.24668
-0.22178
-0.15401
-0.06501
0.03319
0.13436
0.23487
0.33357
0.42932
0.51350
0.60518
0.68603
0.76181
0.83172
0.89571
0.95546
1.00798
1.05503
1.09827
1.13429
1.16478
1.18974
1.21074
1.22461
1.23293
1.23570
1.23293
1.22461
1.21074
1.18974
1.16478
1.13429
1.09827
1.05503
1.00798

APPENDIX G. COMPARISON OF JONES1 AND JONES2 VALUES OF THE INSIDE INTEGRAL
WITH VAN HOUTEN'S VALUES OF THE INSIDE INTEGRAL

R	VALUE OF INSIDE INTEGRAL		% DIFFERENCE BETWEEN JONES1 AND VAN HOUTEN'S	
	VAN HOUTEN'S	JONES1	JONES2	
-1.50000	0.69758	0.69181	0.69179	1 0.83
-1.45313	0.66847	0.67833	0.67839	2 -1.48
-1.40625	0.66746	0.60559	0.60561	3 -9.27
-1.35938	0.37190	0.37536	0.37535	4 -0.93
-1.31250	0.02912	0.44074	-0.44074	5 -1413.53
-1.26563	-0.41609	-0.29548	-0.29548	6 91.35
-1.21875	2.84182	3.64357	3.64358	7 -28.21
-1.17183	12.47668	8.13610	8.13610	8 34.77
-1.12500	8.91488	8.48982	8.48580	9 4.77
-1.07813	6.96253	6.58171	6.58170	10 5.47
-1.03125	4.88435	4.85099	4.85099	11 0.68
-1.08438	3.38097	3.35730	3.35730	12 0.70
-0.93750	2.05348	2.10854	2.10849	13 -2.68
-0.89063	1.01299	1.06492	1.06489	14 -5.13
-0.84375	0.10356	0.16184	0.16183	15 -56.23
-0.79688	-0.75777	-0.61879	-0.61880	16 16.18
-0.75000	-1.34876	-1.26543	-1.26546	17 6.36
-0.70313	-1.90174	-1.81883	-1.81888	18 4.33
-0.65625	-2.40410	-2.31692	-2.31693	19 3.69
-0.60938	-2.86302	-2.75728	-2.75726	20 3.41
-0.56250	-3.23576	-3.12539	-3.12540	21 3.37
-0.51563	-3.49790	-3.44993	-3.44995	22 1.72
-0.46875	-3.89733	-3.74847	-3.74853	23 2.89
-0.42188	-4.06769	-3.97713	-3.97713	24 3.30
-0.37500	-4.21588	-4.17841	-4.17841	25 1.79
-0.32813	-4.53605	-4.38655	-4.38660	26 2.15
-0.28125	-4.62380	-4.54113	-4.54122	27 2.83
-0.23438	-4.74552	-4.64331	-4.64341	28 2.08
-0.18750	-4.78919	-4.74920	-4.74930	29 1.70
-0.14063	-5.00409	-4.85953	-4.85956	30 1.88
-0.09375	-5.00427	-4.92306	-4.92316	31 1.78
-0.04688	-5.04047	-4.94558	-4.94558	32 1.88
0.00000	-5.04047	-4.94553	-4.94565	33 1.70
0.04688	-5.00042	-4.85958	-4.85969	34 2.89
0.09375	-5.00040	-4.85955	-4.85966	35 2.89
0.14063	-5.00040	-4.85955	-4.85966	36 2.89

0.84
0.16
1.79
3.30
0.89
0.22
3.82
1.37
3.41
3.70
3.63
4.36
6.14
16.28
-56.13
-2.68
0.70
0.68
5.47
34.77
34.79
-28.21
-91.35
-1413.50
-9.27
-1.48
-0.83

-4.74917
 -4.64322
 -4.54106
 -4.438656
 -4.17840
 -3.57706
 -3.74845
 -3.44993
 -3.12535
 -2.75719
 -2.31689
 -1.81887
 -1.26539
 -0.61872
 -0.16184
 1.06493
 2.10854
 3.55732
 4.85099
 6.58171
 8.48975
 13600
 3.64350
 -0.29550
 -0.44073
 -0.37537
 0.60559
 0.67835
 0.69179

0.18750
0.23438
0.28125
0.32813
0.37500
0.42188
0.46875
0.51563
0.56250
0.60938
0.65625
0.70313
0.75000
0.79688
0.84375
0.89063
0.93750
0.98438
1.03125
1.07813
1.12500
1.17188
1.21875
1.26563
1.31250
1.35938
1.40625
1.45313
1.50000

REFERENCES

1. Gabor, D., "A New Microscopic Principle," Nature 161, 777, 1948.
2. Gabor, D., "Microscopy by Reconstructed Wavefronts," Proceedings of the Royal Society A 197, 454, 1949.
3. Collier, R., Burckhardt, C.B., and Lin, L.H., Optical Holography, Academic Press, New York, 1971.
4. Collins, D., "Measurement of Velocities in Single and Two-Phase Flows," von Karmen Institute for Fluid Dynamics, Lecture Series 54, 19-23 February, 1973.
5. Radley, R.J., Jr. and Havener, A.G., "The Application of Dual Hologram Interferometry to Wind Tunnel Testing," AIAA Paper 73-210, Washington, D.C., 1973.
6. Chapman, D.R., Kuehn, D.M., and Larson, H.K., "Investigation of Separated Flows in Supersonic and Subsonic Streams with Emphasis on the Effect of Transition," NACA TN 3869, 1957.
7. Korst, H.H., "A Theory for Base Pressures in Transonic and Supersonic Flow," ASME Journal of App. Mech. 23, 593-600, 1956.
8. Roache, P.J., "Numerical Solutions of Compressible and Incompressible Laminar Separated Flows," Ph.D. Thesis, University of Notre Dame, 1968, University Microfilms, Inc., Ann Arbor, Michigan, 1970.
9. Wazzan, A.R., "Review of Recent Developments in Turbulent Supersonic Base Flow," AIAA Journal 3, 1135, 1965.
10. Schlichting, H., Boundary Layer Theory, 6th ed., 26,41, McGraw-Hill Book Co., New York, N.Y., 1968.
11. Nassenstein, H., et al, Engineering Uses of Holography, 25, Cambridge University Press, 1970.
12. Sweeney, D.W., "Interferometric Measurement of Three-Dimensional Temperature Fields," Ph.D. Thesis, University of Michigan, 1972.
13. Matulka, R.D., "The Application of Holographic Interferometry to the Determination of Asymmetric Three-Dimensional Density Field in Free Jet Flow," Ph.D. Thesis, Naval Postgraduate School, Monterey, Ca., 1970.
14. Rowley, P., "Quantitative Interpretation of Three-Dimensional Weakly Refractive Phase Objects Using Holographic Interferometry," Journal of the American Optical Society 59, 1496, 1969.

15. Junginger, H.G. and van Haeringer, W., "Calculation of Three-Dimensional Refractive Index Field using Phase Integrals," Optics Communications 5, 1, 1972.
16. Sweeney, D.W., "Interferometric Measurement of Three-Dimensional Temperature Fields," Ph.D. Thesis, University of Michigan, 1972.
17. Van Houten, P., "The Application of Holographic Interferometry to the Determination of Discontinuous Three-Dimensional Density Fields," A. E. Thesis, Naval Postgraduate School, Monterey, Ca., 1972.
18. Froberg, C., Introduction to Numerical Analysis, 195-223, Addison-Wesley Publishing Co., 1965.
19. Bergland, G.D., "A Guided Tour of the Fast Fourier Transform," Bell Telephone Laboratories, Inc., IEEE Spectrum, July, 1969.
20. Brigham, E.O., The Fast Fourier Transform, 198-221, Prentice-Hall, Inc., Englewood Cliffs, New Jersey, 1974.
21. Everett, R., "Experimental Techniques in Holographic Interferometry," Naval Postgraduate School, Monterey, Ca., 1973.
22. Singleton, R.C., "An Algorithm for Computing the Mixed Radix Fast Fourier Transform," IEEE Transactions on Audio and Electroacoustics AU17-2, June, 1969.

INITIAL DISTRIBUTION LIST

	No. Copies
1. Defense Documentation Center Cameron Station Alexandria, Virginia 22314	2
2. Library (Code 0212) Naval Postgraduate School Monterey, California 93940	2
3. Chairman Department of Aeronautics Code 57 Naval Postgraduate School Monterey, California 93940	1
4. Professor D.J. Collins Department of Aeronautics Code 57C0 Naval Postgraduate School Monterey, California 93940	2
5. LT Harland W. Jones, Jr., USN Air Department USS America CVA-66 FPO New York, New York	1

REPORT DOCUMENTATION PAGE		READ INSTRUCTIONS BEFORE COMPLETING FORM
1. REPORT NUMBER	2. GOVT ACCESSION NO.	3. RECIPIENT'S CATALOG NUMBER
4. TITLE (and Subtitle) Application of Holographic Interferometry to a Supersonic Flow Visualization of a Rear-Facing Step and Application of Fast Fourier Transform Methods to Current Data Reduction Techniques		5. TYPE OF REPORT & PERIOD COVERED Master's Thesis; March 1974
		6. PERFORMING ORG. REPORT NUMBER
7. AUTHOR(s) Harland Wilber Jones, Jr.		8. CONTRACT OR GRANT NUMBER(s)
9. PERFORMING ORGANIZATION NAME AND ADDRESS Naval Postgraduate School Monterey, California 93940		10. PROGRAM ELEMENT, PROJECT, TASK AREA & WORK UNIT NUMBERS
11. CONTROLLING OFFICE NAME AND ADDRESS Naval Postgraduate School Monterey, California 93940		12. REPORT DATE March 1974
		13. NUMBER OF PAGES 90
14. MONITORING AGENCY NAME & ADDRESS (if different from Controlling Office) Naval Postgraduate School Monterey, California 93940		15. SECURITY CLASS. (of this report) Unclassified
		15a. DECLASSIFICATION/DOWNGRADING SCHEDULE
16. DISTRIBUTION STATEMENT (of this Report) Approved for public release; distribution unlimited.		
17. DISTRIBUTION STATEMENT (of the abstract entered in Block 20, if different from Report)		
18. SUPPLEMENTARY NOTES		
19. KEY WORDS (Continue on reverse side if necessary and identify by block number) Holographic Interferometry Fast Fourier Transform Interferometric Measurement Supersonic Flow Visualization Rear-Facing Step Flow		
20. ABSTRACT (Continue on reverse side if necessary and identify by block number) The successful application of holographic interferometry to the study of three-dimensional density fields around bodies in wind tunnel experiments has been reported in the literature along with the associated mathematical reduction processes for the basic interferometric equation. The present report has extended the application of holography as a flow visualization technique by investigating Mach 2.8 flow over a rear-facing 1/8 in. step. Two single-exposed holograms of the model and two double-		

20. (cont'd)

exposed frozen fringe holographic interferograms of the flow were created.

Fast Fourier Transform (FFT) methods have been reported as significantly reducing computational time to obtain discrete and inverse discrete Fourier transforms. Two computer programs were designed to apply FFT methods to the Fourier transform approach to the basic interferometric equation. These programs were used to investigate an alternate way to calculate the value of the inside integral. Total agreement was not found, and further analysis as to the accuracy of each method is needed.

20970

Thesis
J7195
c.1

Jones

150868

Application of holo-
graphic interferometry
to supersonic flow
visualization of a rear-
facing step and applica-
tion of fast fourier
transform methods to
current data reduction
techniques.

Th
J
c

20970

Thesis
J7195
c.1

Jones

150868

Application of holo-
graphic interferometry
to supersonic flow
visualization of a rear-
facing step and applica-
tion of fast fourier
transform methods to
current data reduction
techniques.

thesJ7195

Application of holographic interferometr



3 2768 002 10589 2

DUDLEY KNOX LIBRARY